



DEGREE PROJECT IN THE BUILT ENVIRONMENT,
SECOND CYCLE, 30 CREDITS
STOCKHOLM, SWEDEN 2016

Photogrammetric point cloud generation and surface interpolation for change detection

JOLINE BERGSJÖ

KTH ROYAL INSTITUTE OF TECHNOLOGY
SCHOOL OF ARCHITECTURE AND THE BUILT ENVIRONMENT

ACKNOWLEDGEMENTS

This paper is the result of my master thesis work at the master degree in Transport and Geoinformation Technology Engineering at the Royal Institute of Technology(KTH), Stockholm, Sweden.

I would like to foremost express my gratitude to my supervisor at METRIA Torbjörn Rost for your guidance, expertise and support. I would also like to thank METRIA for lending me a place to work, data sets and software licenses as well as everyone working in METRIAs Stockholm office for ideas and guidance, especially Manuela Alvarez.

I am very grateful to the municipality of Botkyrka who lent me data sets as well as Timo Ikola at ERDAS, Daniel Åkerman and Håkan Wiman at Spacemetric who helped me with licenses, installations and software support during this thesis work.

Finally, I would like to thank my supervisor at KTH Milan Horemuz for guidance, constructive comments and for leading me in the right direction throughout my work.

LIST OF FIGURES

Figure 1 and 2. Photogrammetric normal case and photogrammetric image- and model coordinate systems (Boberg, 2013)

Figure 3. Study area in the municipality of Botkyrka

Figure 4. Keystone components (Spacemetric, 2016)

Figure 5. Flowchart of the methodology

Figure 6. Bare ground feature mask

Figure 7. Forest feature mask

Figure 8. Areas used as representation for the features bare ground and forest.

Figure 9. Ground truth data

Figure 10. Neighbor definition for the ERDAS clump function. Four and eighth neighbors respectively

Figure 11. 3D view of a point cloud-tile from Keystone showing two houses and sparse forest. Points are colored by elevation.

Figure 12. Profile view of deciduous and coniferous forest. NNH point cloud shown in green and Keystone point cloud shown in red

Figure 13. 3D-view of one point cloud-tile generated through ERDAS showing bare ground and forest. Points colored by elevation.

Figure 14. Coniferous and deciduous forest. NNH point cloud shown in green and ERDAS point cloud shown in green

Figure 15. Bare ground and coniferous forest, NNH point cloud shown in green and ERDAS point cloud shown in green

Figure 16. 3D-view of subsection of interpolated surface Keystone with percentile 50(p50) and 2-meter resolution, the point cloud is colored by elevation

Figure 17. Profile view of surfaces interpolated from Keystone point cloud. Keystone point cloud is shown in grey. The different percentiles are shown as following; 50th percentile shown in turquoise, 90th percentile shown in green, 95th percentile shown in red and

Figure 18. Profile view of surfaces interpolated from ERDAS point cloud. 2-meter resolution shown in orange, 5 meter resolution shown in green and 10 meter resolution shown in turquoise

Figure 19. Tilt-check for Keystone surface

Figure 20. Tilt-check for ERDAS Surface

Figure 21. Change detection image between the surface interpolated with the 50th percentile from the Keystone point cloud and NNH-surface, resolution 2 meters. No classes.

Figure 22. Change detection image between the surface interpolated with the 50th percentile from the Keystone point cloud and NNH-surface, resolution 2 meters. Values are classified.

Figure 23. Change detection image between a surface interpolated with the 50th percentile from the Keystone point cloud and NNH-surface, resolution 2 meters. Values are classified and single pixels are eliminated.

Figure 24. Deforestation in Figure 20 circle 1, the area in 2011 and the area in 2014.

Figure 25. Change detection image between the surfaces interpolated with the 50th percentile from the Keystone point cloud and NNH-surface in different resolutions. Only the deforestation class is shown.

Figure 26. No deforestation in Figure 22 circle 3, the area in 2011 and the area in 2014.

Figure 27. Change detection image between the surfaces interpolated with the 50th, 95th and 100th percentile from the Keystone point cloud and NNH-surface, resolution 2 meters.

Figure 28. Deciduous forest in study area that isn't registered in the photogrammetric generated point clouds

Figure 29. One GTD segment over a surface with 10-meter resolution

LIST OF TABLES

Table 1. Accuracy of generated point clouds in relation to the NNH-point cloud

Table 2. GTD extracted from difference images between generated surfaces and interpolated (with p95) surface of NNH point cloud.

Table 3. Accuracy of image matched surfaces in relation to NNH point cloud for bare ground feature

Table 4. Accuracy of image matched surfaces in relation to NNH point cloud for forest feature

Table 5. Accuracy for noise reduced surfaces of forest feature interpolated with the 100th percentile from Keystone point cloud

LIST OF CHARTS

Chart 1. Median value for difference image between image matched surfaces and image matched point cloud for bare ground feature

Chart 2. Median value for difference image between image matched surfaces and image matched point cloud for forest feature

Chart 3. Median for differential images of bare ground feature

Chart 4. Median for differential image of forest feature

LIST OF ABBREVIATIONS

DEM – Digital Elevation Model

DSM - Digital Surface Model

ALS - Airborne Laser Scanning

TLS – Terrestrial Laser Scanning

LiDAR – Light Detection and Ranging

NNH – New National Height model

GCP – Ground Control Point

FBM – Feature based Matching

GBM – Global based Matching

SGM – Semi-Global based Matching

SfM – Structure-from-Motion

MI – Mutual Information

IMU – Inertial Measurement Unit

INS – Inertial Navigation System

ABSTRACT

In recent years the science revolving image matching algorithms has gotten an upswing mostly due to its benefits in computer vision. This has led to new opportunities for photogrammetric methods to compete with LiDAR data when it comes to 3D-point clouds and generating surface models. In Sweden a project to create a high resolution national height model started in 2009 and today almost the entirety of Sweden has been scanned with LiDAR sensors. The objective for this project is to achieve a height model with high spatial resolution and high accuracy in height. As for today no update of this model is planned in the project so it's up to each municipality or company who needs a recent height model to update themselves. This thesis aims to investigate the benefits and shortcomings of using photogrammetric measures for generating and updating surface models. Two image matching software are used, ERDAS photogrammetry and Spacemetric Keystone, to generate a 3D point cloud of a rural area in Botkyrka municipality. The point clouds are interpolated into surface models using different interpolation percentiles and different resolutions.

The photogrammetric point clouds are evaluated on how well they fit a reference point cloud, the surfaces are evaluated on how they are affected by the different interpolation percentiles and image resolutions. An analysis to see if the accuracy improves when the point cloud is interpolated into a surface. The result shows that photogrammetric point clouds follows the profile of the ground well but contains a lot of noise in the forest covered areas. A lower image resolution improves the accuracy for the forest feature in the surfaces. The results also show that noise-reduction is essential to generate a surface with decent accuracy. Furthermore, the results identify problem areas in dry deciduous forest where the photogrammetric method fails to capture the forest.

SAMMANFATTNING

På senare tid har vetenskapen kring bildmatchningsalgoritmer tagit fart, till stor del tack vare vetenskapsområdet 'computer vision'. Detta har lett till nya möjligheter för fotogrammetriska metoder att konkurrera med laser-data när det kommer till 3D-punktmoln och att skapa ytmodeller. I Sverige idag genomförs ett projekt sedan 2009 där man ämnar att skapa en noggrann höjdmodell över hela Sverige med hjälp att att skanna av Sverige med flygburen laser-skanning. Målet med projektet är att skapa en högupplöst höjdmodell över Sverige med hög noggrannhet i höjd. Ingen uppdatering av denna höjdmodell är planerad och det är därför upp till var kommun eller företag att själv uppdatera det område som har förändrats om behovet finns. Arbetet i den här rapporten ämnar att undersöka fördelar och nackdelar med att använda fotogrammetri i ändamålet att skapa eller uppdatera en höjdmodell. Två mjukvaror för att generera punktmoln via fotogrammetri användes; 'ERDAS Photogrammetry' och 'Spacemetric Keystone'. Två 3D-punktmoln skapades över ett landsbygdsområde i Botkyrka kommun. Punktmolnen interpolerades sedan till yt-modeller genom att använda olika interpolationspercentiler och olika bildupplösningar.

De fotogrammetriska punktmolnen utvärderas utefter hur väl de överensstämmer ett referenspunktmoln, ytorna utvärderas utefter hur de påverkats av de olika interpolationspercentilerna och bildupplösningarna samt en analys för att se om noggrannheten blir bättre hos den interpolerade ytan än hos punktmolnet det är generat från. Resultaten visar att fotogrammetriska punktmoln väl följer markprofilen men att punktmolnet är brusigt i skogsområden. Lägre bildupplösning ger i skogsområden en högre noggrannhet än högre bildupplösning. Resultaten visar även att brus-reducering är viktigt för att uppnå tillfredsställande resultat. Resultatet identifierar även problemområden såsom torr lövskog där den fotogrammetriskt framtagna yt-modellerna inte registrerar lövskogen. Slutligen görs en förändringsanalys i syftet att försöka peka på områden som behöver uppdatering.

TABLE OF CONTENTS

1. Introduction	8
1.1 Background	8
1.2 Objective.....	9
1.3 Scope and limitation.....	9
2. Review of literature and basic concepts	10
2.1 Stereo-photogrammetry	10
2.1.1 Image matching algorithms	12
2.2 Air-borne LiDAR	14
2.3 Properties of 3D point cloud	15
2.3.1 LiDAR generated point cloud	15
2.3.2 Image matching generated point cloud	15
2.4 Digital Elevation Model (DEM).....	15
2.5 National Height model (NNH)	16
2.6 Previous comparative work of others.....	16
3. Study area and Data description	19
3.1 Study area	19
3.2 Data	20
3.2.1 Airborne imagery	20
3.2.2 Other data	20
4. Software.....	21
4.1 Image matching software	21
4.1.1 Keystone.....	21
4.1.2 ERDAS imagine.....	21
4.2 LAStools	22
4.3 ArcGIS.....	22
4.4 Fugroviewer	22
5. Methodology.....	23
5.1 Image matching.....	23
5.1.1 Keystone.....	23
5.1.2 ERDAS Imagine.....	24
5.2 Create surface model	24
5.2.1 Image matched surface models.....	24
5.2.2 NNH surface models.....	25
5.3 Analytical support and determination of accuracy level.....	25
5.3.1 Feature masks	25
5.3.2 Surface models statistics	26
5.3.3 Systematic errors	27
5.4 Change detection	29
5.5 Noise reduction and elimination of gross error	30
6. Result and Analysis	31
6.1 Image matched point clouds.....	31
6.1.1 Keystone	31

6.1.2	ERDAS Imagine.....	32
6.1.3	Point cloud accuracy	34
6.2	Image matched surface models	34
6.2.1	Fit to the source point cloud.....	36
6.2.2	Systematic error.....	39
6.2.3	Surface accuracy assessment	41
6.2.4	Noise reduced surface	44
6.3	Change detection	44
7	Discussion	48
8	Conclusions.....	52
9	Recommendations and future studies	52
	References	54

1. INTRODUCTION

1.1 BACKGROUND

Digital Elevation Models (DEM), Digital Surface Models (DSM) are height models which have been produced and used for decades and the technique has developed throughout the years. The models are 3D or 2.5D representation of a surface and are used for example in environmental change monitoring, volume assessment of forestry and 3D-reconstruction. Initially the models were created almost exclusively by using aerial photogrammetry. The technique uses trigonometric relationships of overlapping images to calculate the position of points, resulting in a point cloud. At first the technique was carried out manually and eventually with modern technique automatically. Since mid-nineties airborne laser scanning (ALS) has become more available and consequently gained popularity due to several factors, the utmost one being the accuracy in height it provides. ALS uses a LiDAR (Light Detection and Ranging) sensor to efficiently collect height information from a surface that is stored as a point in a point cloud. Since the sensor is active it does not require sun light and it can penetrate vegetation which allows information of both the ground as well as the coverage of it.

The need for accurate DSMs and DTMs are increasing in various fields such as city planning, forest monitoring and decision support. The utility and accessibility of ALS has nourished the interest to find alternative techniques to retrieve surface height information and has again opened the door for photogrammetry. Up-to-date advances in computer processing and algorithm development have spread new light on photogrammetric techniques that can process much faster and with higher accuracy. The transition from film to digital data storage has increased the radiometric resolution of images which allows for more complex matching algorithms.

ALS in comparison to aerial photography requires lower altitudes and slower flying speeds when collecting the data (Leberl, et al., 2010). This results in more flying hours for ALS surveying in comparison to aerial photography hence higher data collection costs. Still, aerial photography is dependent on sun angles as well as the weather which limits the collection opportunities.

ALS is often used to monitor the environment and for climate decision support, the DSM generated for these purposes are a snapshot of the surfaces if no updates are planned. An example of this is the project to create a New National Height model of Sweden, which purpose is to fit the growing needs for accurate height information for climate adjustment measures (Lantmäteriet, 2016). The project started in 2009 and is planned to be finished by 2016/2017, no updates are planned. This height model will soon have a low temporal resolution. One way to update this model without ALS is to update it with photogrammetric methods using airborne photography which is collected more frequently in Swedish municipalities.

Photogrammetric methods generate dense point clouds but with more erroneous points than LiDAR. The errors are due to mismatched feature points that leads to false trigonometric relationships which leads to erroneous points. The point clouds are usually, due to these properties, noisy. Different interpolation percentiles of such point cloud will give different properties in the generated surface. A high percentile will generate a surface that in general is

higher than a surface interpolated with a lower percentile. Depending on the properties of the point cloud, different percentiles can exclude outliers and enhance the overall accuracy of the surface. Different spatial resolutions can also affect the surface. A surface interpolated with a high resolution will have fewer points in each cell in comparison to a surface interpolated with a lower resolution.

This thesis deals with point clouds generated through image matching and investigate its benefits and shortcomings in terms of being used to create surface models. It creates DSMs that are evaluated on how well they fit the image matched point cloud as well as excluding outliers from the point cloud. Finally, an assessment of the accuracy achieved in the DSMs is carried out in order to establish what kind of temporal change that can be detected using photogrammetry to update a DSM.

1.2 OBJECTIVE

Photogrammetric methods generate dense point clouds but with more erroneous points than a point cloud generated from a LiDAR-sensor. The idea that motivated this thesis is that when interpolating dense point clouds from image matching you can receive a higher accuracy than in each point of the point cloud. The overall accuracy of the interpolated surfaces is thought to be affected by different interpolation percentiles and image resolutions.

In this thesis photogrammetric point clouds will be generated and evaluated on their accuracy in comparison to a reference point cloud. Different interpolation percentiles and image resolutions will be used to generate surface models from said point clouds. The surfaces will be evaluated on how they fit the reference source cloud and how the different percentiles and image resolutions affect the surfaces are assessed. Finally, the accuracy of the point cloud will be compared to the accuracy of the surfaces to see if the accuracy of a point cloud can improve when interpolated into a surface.

1.3 SCOPE AND LIMITATION

The scope of this thesis includes two image matching software for generating point clouds, however not much attention is put on comparing theses software. The interpolation variation techniques in this thesis is limited to different percentiles and different image resolution. The study area is limited to a rural area mostly covering fields and forest. Some houses are included in the study are but no urban areas.

2. REVIEW OF LITERATURE AND BASIC CONCEPTS

2.1 STEREO-PHOTOGRAMMETRY

Stereo vision enables 3-dimentional experience of objects in the 2D-plane and can be used for photogrammetric measurements and 3D-cloud construction. Our eyes view objects from slightly different perspective and when we move, an object is displaced in relation to the observing point; this displacement is in photogrammetry called horizontal- or x-parallax (Philpot & Philipson, 2012). By using two images that overlap, depth perception can be recreated. This recreation gives an opportunity to measure objects within the images and through trigonometric calculations 3D-points can be extracted. The workflow of extraction of 3D-coordinates from 2D images will be explained in this chapter.

In order to retrieve 3D-point information three orientations need to be determined; interior, relative and absolute orientation. The interior orientation parameters include the coordinates of image center of the camera, the focal length, the image frame resolution and the camera constant (distance between the image plane center and the camera optical center) (Schenk, 2005). In the image, object coordinates are referenced to an image coordinate system. The coordinates for the first image are designated as x' and y' and the coordinates for the second image are designated as x'' and y'' (Boberg, 2013). When the images are oriented relative to each other, their coordinates can be transformed into model coordinates. The model coordinate system can with help of absolute orientation be transformed into any known exterior reference system, such as SWEREF99, which is used in this study.

Relative orientation offers a possibility to create a stereo model that holds 3D-point information in a local coordinate system. The y-parallax is calculated using $P_y = y' - y''$, i.e. the differences between the feature position in each image perpendicular to the flight direction (Boberg, 2013). If the y-parallax is zero it indicates that the images are taken on a perfect line of flight (i.e. the plane is flying perfectly straight and perfectly parallel with the ground) and no relative orientation is necessary, this is never the case in reality and relative orientation is needed. The orientation is done mathematically by calculating the rotation matrices that rotate the two vectors ((O1, P) and (O2, P) in Figure 2), which goes from respective camera center through the feature in the respective images until they intersect with each other, meaning the y-parallax is zero.

Imperfections in the relative orientation is always existent and small errors in x-parallax can occur which directly affects the height measurements in the stereo model.

When the images are oriented relative to each other and the y-parallaxes is zero the model coordinates can be calculated. The coordinates are obtained from trigonometric calculations using the ratio of sides of uniform triangles, see Equations (1), (2) and (3). Note that the images z-coordinate is the camera constant c , which is negative in all airborne imagery. The variable b is the base, usually the distance from each camera center, for visualization see Figure 1.

$$\mathbf{x}: \frac{x}{x'} = \frac{z}{-c} \rightarrow \mathbf{x} = x' \times \frac{z}{-c} \quad (1)$$

$$\mathbf{y}: \frac{y}{y'} = \frac{y}{y''} = \frac{z}{-c} \rightarrow \mathbf{y} = y' \times \frac{z}{-c} = y'' \times \frac{z}{-c} \quad (2)$$

$$\mathbf{z}: \frac{z}{-c} = \frac{b}{x' - x''} \rightarrow \mathbf{z} = -c \times \frac{b}{x' - x''} \quad (3)$$

Since $P_x = x' - x''$ then:

$$\mathbf{z} = -c \times \frac{b}{P_x}$$

Substituting z in Equations (1) and (2) give:

$$x = x' \times \frac{b}{P_x} \text{ and } y = y' \times \frac{b}{P_x}$$

Equations (1),(2) and (3) and the substitutions are from (Boberg, 2013).

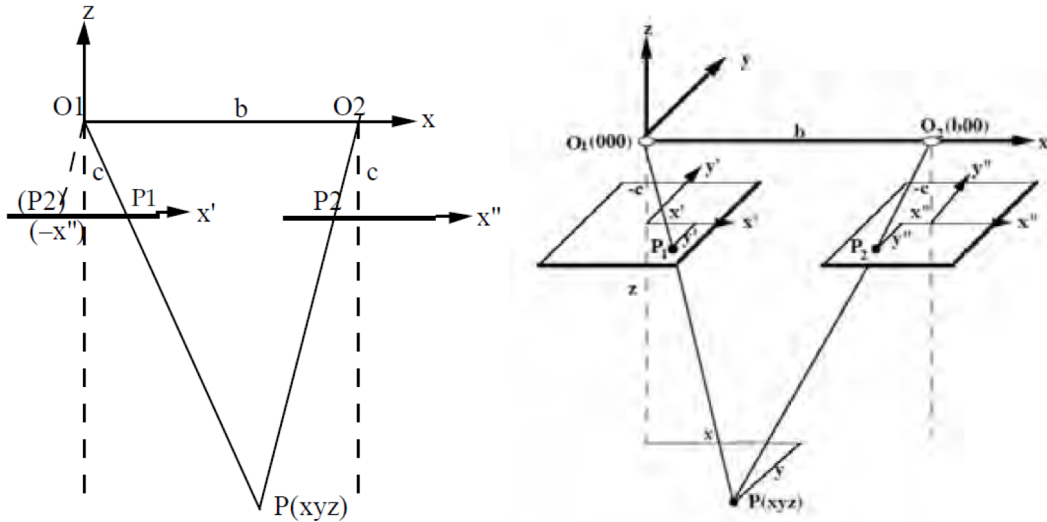


FIGURE 1 AND 2. PHOTOGRAHMETRIC NORMAL CASE AND PHOTOGRAHMETRIC IMAGE- AND MODEL COORDINATE SYSTEMS (BOBERG, 2013)

The model coordinates hold the point information but the model is given in a local system that floats freely in space. Transformation and translation parameters are therefore calculated through absolute orientation to fit the local coordinates to known exterior coordinates.

The absolute orientation is performed using a uniformed Helmert-transformation which requires seven parameters to perform; Three translation parameters (X_O, Y_O, Z_O) to get the position in relation to the ground, three angles (Ω, ϕ, K) that rotates the model coordinates around their axes until they are levelled with the axis of the known coordinate system and finally a scale factor m that scales the system according to the known system. The scale factor is calculated as $m = \frac{d}{d'}$ where d is the distance in known coordinate system and d' is the same distance in the model coordinate system. (Boberg, 2013)

To solve these parameters at least seven equations are needed. These equations can be set up using known ground control points whose model coordinates are calculated. A minimum of two ground control points with known horizontal position and three ground points with known vertical position is needed, but usually more points are used to over determine the transformation parameters.

Collection of airborne imagery is usually done in so called blocks, where the flight path goes back and forth in parallel paths that overlap. This allows for a technique called block triangulation to be used. Block triangulation requires a small amount of known ground control points, where absolute orientation in every image pair would require a large amount of ground control points. Block triangulation uses ground control points that are visible in two to six images and a number of connection points that are visible in several images. The connection points are clearly visible features in the images that can be matched into feature pairs and is used for relative orientation between the images. This means that relative and absolute orientation is substituted for block triangulation. Information of the airplane and camera position is used for exterior orientation together with collinearity equations to orient the images, the large non-linear equation system is solved by using the least square method (after linearization) and the over determination of the equation system generates a decent stereo

model. If no ground control points are accessible, block triangulation can be performed with only connection points, which would generate a stereo model in a local model coordinate system where all points would be related to the image center of one image. If GPS information is acquired when collecting the images, it can be used to orient the stereo model to an exterior coordinate system.

Block triangulation is carried out automatically where finding distinct connection point pairs is of importance. A great deal of algorithms is developed for this purpose. In the following section image matching algorithms will be described further.

2.1.1 IMAGE MATCHING ALGORITHMS

Image matching algorithm is used predominantly in photogrammetry and computer vision but also other fields of science. Feature based matching (FBM) was first developed in mid-eighties; since then it has gone through numerous of modifications and been implemented in several software applications. It has become a trustworthy algorithm for image matching. More recently global based matching algorithms have become popular since it has shown great result, especially for sub-pixel accuracy (Szeliski, 2011). The newer and today most utilized is Global based matching (GBM) and Semi-global based matching (SGM).

Even though the techniques have been developed during a long period of time the algorithms usually performs all of, or subsets of, four steps; Determine the cost and cost aggregation, determine the disparity and finally refine the disparity (Scharstein & Szeliski, 2001).

The most eminent image matching algorithms will be presented in this chapter.

Feature based matching (FBM)

The feature based approach aims to extract feature points in overlapping images and then find matching pairs. An interest operator is used to find distinctive points in the separate images. The interest operator is an algorithm that is used to signal points or regions in an image that might be useful for image matching; there are several different algorithms such as the Harris Interest operator (Harris & Stephens, 1988) that identify corners and the Förstner interest operator (Förstner & Gulch, 1987) that identify corners and circular image features. From the identified points a preliminary list of candidate pairs is created using similarity measures. The preliminary list of candidate pairs is trimmed down using a global- or object model. A global- or object model can be a 3D model or be withdrawn from the mapping function between the overlapping images and then be interpreted as an 3D-model (Barnard & Thompson, 1980). In the first step distinct points are selected based on several factors. For example, local separability is achieved by only choosing pixels that are different from their neighboring pixels. In the second step prior knowledge is used to trim down the list of point pairs. For example, the maximum parallax is used to determine the likeliness of the points corresponding to each other. Finally the global consistency is achieved by implementing a global- or object model that the data is fitted to, the consistency is considered the fit of data with respect to the global- or object model (Förstner, 1984).

The FBM algorithm has been developed and altered in different studies and software applications. Shapiro and Brady (1992) find feature correspondence between feature points using their eigenvector properties. The similarity of the eigenvector properties is summarized in an association matrix, where the correspondence between feature points are well defined.

Global based matching (GBM)

Global algorithms first assume smoothness in the images and then proceed to solve a global optimization problem. The smoothness is often restricted to only measure the difference between neighboring disparities with the purpose of keeping the optimization computation manageable. (Szeliski, 2011)

Global based matching is good to use for solving inverse problems, a problem when you try to recover a surface from an ill-posed data set. A data set is ill-posed when many surfaces can fit the data. The technique calculates a “continuous global energy function”. This energy function describes how well the disparity image agrees with the input image. The function is optimized to find the solution that gives the lowest global energy. The lowest global energy indicates the best fit of the datasets. (Szeliski, 2011)

Semi-Global based matching (SGM)

Semi-global matching combines global based matching with local methods such as feature based methods. The method has proven to generate accurate pixel-wise matching with low runtime (Hirschmuller, 2011).

The algorithm utilizes the smoothness constraint of global matching algorithms but take local disparities into consideration by performing pixel-wise matching. The algorithm works on images with exterior and interior orientation. If the image is not rectified it creates epipolar lines and assumes that matching points lie on the same horizontal line. (Dall'asta & Roncella, 2014)

The matching cost is calculated for a pair of pixels often using Mutual Information (MI), but other cost calculations can be used. MI measures the alignment of a model using the uncertainty in a probability density function, see Equation (4) where H represents the entropy (probability that a system will take a certain form) for respective image and the joint entropy for both images. The amount of uncertainty is also called Entropy, each image in the stereo pair has an entropy-value and the combination of the images has an entropy-value. Mutual information is the difference between the entropy of each image and the joint entropy. (Hirschmuller, 2008)

$$MI_{I_1, I_2} = H_{I_1} + H_{I_2} - H_{I_1, I_2} \quad (4)$$

The uncertainty is only measured for un-occluded pixels. A disparity map can be used to align the images, if they are aligned well, MI is optimized. To find the entropy, MI uses the histogram of each image and a joint histogram for the joint entropy. This results in MI working well on images with radiometric differences. However, it does not work well with increasing radiometric depth (i.e 12 or higher bit instead of 8) or increasing local radiometric differencing such as vignetting. Other cost calculation algorithms can be used, for example census (see e.g. Humenberger, Engelke & Kubinger, 2010), but studies have proven MI to be a well working algorithm for SGM. (Hirschmuller, 2011)

The MI is used to calculate the matching cost for each pixel and its disparity (The pixel value of the matched pixel in the second image) according to Equation (5) where p is the pixel value, D_p is the disparity pixel and h is the entropy. (Hirschmuller, 2008)

$$-C(p, D_p) = h_{I_1}(p) + h_{I_2}(D_p) - h_{I_1, I_2}(p, D_p) \quad (5)$$

Pixel-wise cost calculations are naturally ambiguous (Hirschmuller, 2008). To solve these ambiguities a cost aggregation approach using a global energy function (smoothness constraint) is utilized.

The cost aggregation is performed path wise. For each pixel eight paths from all directions of the pixel are generated. Each path carries the information of the aggregated cost for reaching a pixel with a certain disparity. The cost for each pixel-disparity pair is summarized over the eight paths and thereafter the disparity with the lowest cost is chosen for each pixel. (Hirschmuller, 2011)

SGM has shown to be tolerant against radiometric differences and pixel-wise matching is done accurately on pixel-, and sub-pixel-, level. It also has a low runtime in comparison to other techniques with similar results. (Hirschmuller, 2008)

2.2 AIR-BORNE LiDAR

The Air-borne LiDAR, also called Air-borne Laser Scanning (ALS), data has multiple usage including city modeling, coastal mapping, corridor mapping, canopy mapping and of course generation of elevation and surface models (Horemuz, 2015).

LiDAR is an acronym for “Light Detection and ranging” and it is using an active-sensing laser beam in order to measure the distance(ranging) between the sensor and the spot the beam illuminates. By doing this on a large amount of spots a point cloud can be generated (Wehr & Lohr, 1999). The range measurements can either be done using a pulse-based method or a phase-based method. The phase-based method transmits a continuous signal and measures the phase-difference between that signal and the for the returning backscatter-signal. In ALS the pulse-based method is usually used. The pulse-based method sends out a pulse of light and then clock the time it takes for that signal to return to the sensor. Since the speed of light is known the range (or distance) can be calculated from the equation for traveling time of a pulse:

$$t_L = 2 \frac{R}{c} \quad (6)$$

Where t_L is the time it takes for the pulse to return, c is the speed of light and R is the range (Wehr & Lohr, 1999)

The scanner measurements are a measure of the distance from the laser scanner to the point on the earth surface. In order to compute the 3D-position of the points the position and orientation of the laser scanner must be known in relation to a known coordinate system at some time during the scan-sequence (Wehr & Lohr, 1999). The position is known with help of a GPS that tracks the plane that carries the laser scanner. On the plane there is also an Inertial Measurement Unit (IMU). An IMU measures the angular rate and the specific force of a body, in this case the airplane (King, 1989). It does this by using gyroscopes and accelerometers. With the information from the IMU transformation and translation parameters can be calculated in order to find the position of each scanned point in any known reference system.

Errors associated with air-borne LiDAR include sensor associated errors, such as synchronization errors, errors in relative position etc. Environmental conditions such as turbulence, engine vibrations and flying height has a great impact on the point cloud, and errors in those aspects need to be minimized. Furthermore, Air-borne LiDAR is dependent on a GPS and an INS, therefore signal propagation errors, offset errors or phase and pseudo range measurement errors can cause severe problems. (Horemuz, 2015)

2.3 PROPERTIES OF 3D POINT CLOUD

3D point clouds can be generated through several different procedures that all generates different properties for the respective point cloud. In this thesis point clouds generated through LiDAR measurement and image matching is utilized, the varied properties of the respective point clouds are given in this chapter.

2.3.1 *LiDAR GENERATED POINT CLOUD*

LiDAR is an active sensor which gives the possibility to collect data at any light condition. LiDAR points often contain intensity information, which can be useful when analyzing the data. The accuracy of each point is often better in height than in the horizontal plane, up to 5 cm in height and 10-15 cm I horizontal position (Gehrke, S., et al., 2010). There can be errors in the point cloud due to unhandled atmospheric conditions when retrieving the data. LiDAR data is sensitive to water, the laser beam can reflect away on the water and return signal can not be registered. If there are puddles of water on the ground it can affect the point density in that area. The best surface to collect LiDAR data is a flat and dry surface, for example fields with short grass or roads.

The laser beam penetrates vegetation and therefore has the ability to capture ground data even through dense forest canopy. However, the type and state of the vegetation also affects the point density and accuracy. For example, if the forest has a high density in the top side of the canopy it often gives low point density with high accuracy. This is because the compact canopies don't let enough light through for the vegetation on the ground to grow big, hence a flat surface. If the canopy lets more light through the vegetation on the ground it will be harder to penetrate. During spring time when the vegetation on the ground has not yet grown to its fullest and the canopies have started to burst is a good time to collect LiDAR data (Boberg, 2013).

The point density in the cloud is determined by the velocity of the aircraft carrying the scanner and the flying height. The lower the flying height and the slower the velocity the better the resolution of the point cloud. This means that ALS can, if details are important, be quite time consuming.

2.3.2 *IMAGE MATCHING GENERATED POINT CLOUD*

A contrary to LiDAR data, image matched point clouds can not penetrate vegetation. In order for a matched point to be on the ground, a tie point on the ground needs to have been found in at least two overlapping images. Therefore, it is hard to collect ground information in dense forests. Airborne photography uses a passive sensor, meaning it requires external light to capture the ground surface hence the data needs to be collected during daylight (Boberg, 2013). An image matched point can inherit colors from the overlapping imagery, allowing the point cloud to easily be colored which makes it easier to interpret.

Since the sensor is passive and require daylight, it is also sensitive to shadows. Especially shadows in variable features such as forests. The treetops cast shadows on lower parts of the trees and matches can be found in the shadows between treetops making the point cloud lower than the actual forest height. There can also be confusions in the point matching which leads to faulty trigonometry hence gross errors in the point cloud.

The purchase price for the photography equipment is lower than the expense for a laser scanner. With some image matched point clouds, although not for ALS, consumer grade digital cameras is enough to collect the imagery for image matching. (James, et al., 2015)

2.4 DIGITAL ELEVATION MODEL (DEM)

A Digital Elevation Model (DEM) is a model, often a grid, which represents the surface of an area. The DEM contains information of the height of a surface above a reference plane, such

as any ellipsoid or geoid. It can include only the bare ground and no objects on the surface, also called Digital Terrain Model, or the surface with all objects on the ground included, also called Digital Surface Model. A DSM(Digital surface model) can be described as a blanket that is laying on the surface and traces the height of every object as well as the ground while the DTM(Digital terrain model) exclude all objects on top of the bare ground such as houses or forestry. The model is commonly generated through interpolation of Air-borne LiDAR point cloud or point clouds generated through stereo photogrammetry. (Boberg, 2013)

2.5 NATIONAL HEIGHT MODEL (NNH)

Sweden has in recent years used air-borne LiDAR to systematically collect elevation information over the whole territory of Sweden. Today almost the entirety of Sweden is mapped with only the mountain chain in the north-west left. The requirement for the point cloud is to have a point density of at least 0.5 points/m². In order to fulfill this requirement the data is collected with a mean density of 0.9 points/m². The reference systems are SWEREF99 TM for the horizontal plane and RH 2000 for the vertical plane. (Metria, 2016) SWEREF99 TM and RH 2000 are the standard reference systems for Swedish geodata (Lantmäteriet, 2016).

The DEM created from these measurements is called the ‘New National Height model GRID 2+’ (NNH grid 2+). (Geografiska Sverigedata, 2015) The surface model is delivered in ascii or text-file, the resolution is 2 meters and the accuracy in height is higher than 0.5 meter while for solid flat surfaces the accuracy in height is better than 0.1 meter. (Lantmäteriet, 2016)

The objective for producing such highly accurate height model is foremost the growing need for such data when analyzing climate change (e.g. flooding analysis) but also for more specific usages such as mapping of transmitter masts or optimal placement of windmills. As of today no update of the model is planned but investigations on which methods that can be used for such update is in action. (Lantmäteriet, 2016)

2.6 PREVIOUS COMPARATIVE WORK OF OTHERS

In the paper “Comeback of Digital Image Matching” from 2009 Prof. Haala argues for the suitability of image matching as a tool to develop elevation models. In the paper he performs a comparative study using several cameras for optical image collection as well as LiDAR data. The result of the study shows that LiDAR still performs better in generating an elevation model but models generated through image matching also achieve sufficient accuracy to be used for the purpose. The study concludes that the development of digital imagery has significantly increased the quality of elevation models generated from image matching. The study encourages further development of image matching algorithms. (Haala, 2009)

In 2013 the European Spatial Data Research Organization (EuroSDR) initiates an extensive test of photogrammetric software. The test aims to evaluate the quality of the different matching algorithms in terms of accuracy and reliability. The test is achieved by providing two image blocks of two areas with diverse structure to study groups that uses different image matching software in their respective work. The study groups are asked to create a Digital Surface Model (DSM) of the two sites, as well as report on the properties of the hardware used and the time consumption of the process. The result of this study is compiled by prof. Norbert Haala with the objective to provide an insight of image matching software as well as an evaluation the current potential of image based photogrammetric data collection. Due to low temporal resolution in the study areas the reference surface used in the compilation is based on the median of all DSMs created in the test. The results are evaluated on their deviation from the reference surface and visuals are created from both study sites that shows how the different results vary from the reference surface. Profiles of problem areas are also visualized and analyzed. Haala concludes that software tools for detailed and reliable

photogrammetric 3D data capture from airborne imagery clearly have potential. The test sites with moderate resolution and overlap can easily be used to generate a surface model. Most of the runtimes are acceptable, even with standard hardware environment. Haala also points out problem scenarios such as shadows and fine object with size close to the spatial resolution of the image. Furthermore, Haala concludes that improved camera technique would be beneficial since it would generate higher radiometric resolution. (Haala, 2014)

In 2015 on behalf of Lantmäteriet (Swedish surveying authority) GeoXD performed a pilot study evaluating the production of 3D point cloud produced from airborne imagery. Based on The EuroSDR study mentioned earlier the photo matching software used in this study is Photogrammetric Surface Reconstruction from Imagery, *SURE*, and *Match-T*. The study focuses on the accuracy of each point in the point clouds, and do not perform any interpolations to create a surface model. The point clouds are compared with the New National Height model (NNH), a height model generated from airborne laser data, covering large areas of Sweden. The NNH is used as the true height and the point clouds deviation from NNH are considered an error. Several parameters are taken into consideration, for instance the density of the points, the amount of matched points and gross errors. The study concludes that the density of the point cloud does not have a severely large effect on the standard uncertainty, but that a low point density will lose details especially in urban areas. When matching the points, *Match-T* matched almost all points while *SURE* only matched approximately 87% of the points (Westoby, et al., 2015). However, the gross errors are three times the amount in *Match-T* than in *SURE*. Gross errors are considered points that deviate more than one meter from NNH. This is explained by the fact that *SURE* seems to exclude points close to buildings, in shadows or from large slopes. These are areas that the study concludes are areas where gross errors regularly occur (GeoXD AB, 2015).

A recently developed photogrammetric technique for image matching was introduced in 2012 by (Westoby, et al., 2015) and is called Structure-from-Motion (SfM). The technique is a low-cost method for high resolution topographic reconstruction. The main difference from traditional photogrammetric methods is that it does not require a priori knowledge of the camera position or orientation. Instead it requires multiple overlapping images and the orientation of them are solved through automatic matching of keypoints extracted from the images. Keypoints are identified using the SIFT-algorithm, the number of matched keypoints is dependent on the image texture and resolution and the minimum requirement is that a keypoint is visible in at least three images. The Keypoints are matched using the RANSAC (Random Sample Consensus) method. RANSAC is an outlier detection algorithm. It attempts to fit the data into a mathematical model by iteration, the more iterations the higher is the probability that the fitted data contain only inliers (i.e. not outliers). In other linearization methods outliers affect the fitted data, but in RANSAC everything not identified as an inlier does not affect the linearized model (Fischler & Robert, 1981). In this case the keypoints are matched with a certain probability threshold, if the probability for them being a match falls within that threshold they are considered a point-par. Triangulation is then used to determine the 3D point position and manual identification of Ground Control Points (GCPs) are finally used for absolute orientation.

An independent assessment of the SfM was undertaken by comparing it to a survey executed using Terrestrial Laser Scanning (TLS). The TLS data acquisition time was approximately 5 hours while the images for SfM only took approximately 2 hours to collect. The post-processing time for SfM was considerably longer where sparse and dense point cloud generation took 23.5 hours while the post-processing for TLS was around 4 hours. A DEM of difference shows that 94% of overlapping model differences is within -1.0 – 1.0 meters and 86% is within -0.5 – 0.5 meters. Positive differences (SfM is higher than TLS) are seen in areas with exposed rock and negative difference is seen in steep faces. Moderately high

positive difference is seen in homogeneous areas such as dense vegetation, or areas covered by snow or sand. It is concluded that SfM has apparent logistical advantages over TLS but that post-processing time is longer. The technique is a cost effective alternative to both TLS as well as other photogrammetric options and is a practical application in remote or inaccessible regions. (Westoby, et al., 2015)

Gehrke, et al. presents a DSM derivation approach utilizing the SGM algorithm. The result is compared to a DSM generated through LiDAR point cloud. It is found that both LiDAR and SGM generates high density digital surfaces, potentially the SGM gives higher density DSMs, which can ease identification of structures in the data. The comparison displays that the average vertical difference is $0.8 \text{ cm} \pm 5.4 \text{ cm}$. The small standard deviation is interpreted as the result being more accurate than expected for both the LiDAR result and the SGM result. It is concluded that the SGM DSM strongly agrees with the LiDAR DSM. The high point density generated through SGM reveals fine details that LiDAR might not catch, while LiDAR can penetrate canopy and therefore generates a better terrain model. Finally it is stated that when using high resolution imagery SGM-derived DSMs are an alternative to LiDAR-generated DSMs, since the results are sufficient and the data acquisition cost is lower for SGM. (Gehrke, S., et al., 2010)

3. STUDY AREA AND DATA DESCRIPTION

3.1 STUDY AREA

Several features were desirable when searching for study sites in this thesis. The first requirement is that the site contains forest, preferable there should be several forests in different growing phases such as old forest, young forest and young fast-growing forest. There should also be areas of clearings. The different growth state of the forest means that different areas can be used for change analysis and other for accuracy calculations (Since the same data is used for both in this thesis). The clearings are interesting since they offer a large degree of change that should be easy to point out in a change detection analysis.

The second requirement is that there are open areas with a flat surface; such as open grass fields, football fields or parking lots. The third requirement is that the area contains some sort of settlement, building or other infrastructure. The open areas are important since both flat surfaces(fields) and forests are of interest and are looked upon separately and houses offers profiles and objects that are easily distinguished by the eye.

Finally, areas where major changes have occurred since NNH of the area was measured are required. The change can be harvested forest, new buildings or roads or any other type of drastic change in the elevation and usage of the ground.



FIGURE 3. STUDY AREA IN THE MUNICIPALITY OF BOTKYRKA

In the area of Botkyrka a set of images over a rural area has been provided from the municipality of Botkyrka, the area can be seen in Figure 3. Study area in the municipality of Botkyrka. The area contains several areas with open fields. The area also contains old forest, which is located in the center of the image together with newly grown forest. A large clearing is located in the top left corner of the site. There is no settlement but single houses in the area;

also there is no new infrastructure that would have been preferred in the site. In the center of the image there is an area that has been deforested since the data set provided was collected.

3.2 DATA

The data used in this thesis was the images used for image matching, the NNH point cloud and different supportive data layers used to analyze the results. In this chapter the data used will be described further.

3.2.1 AIRBORNE IMAGERY

A total of 18 images, delivered in tif-format, were provided from the municipality of Botkyrka. The images are taken on a flight height of approximately 1300 meters with an overlap of minimum 30 %. The orientation data was given in a separate ori -file. An ori -file is a photogrammetry block file format, also called PATB-format, which have a standardized layout. It contains data of the image ID, the plane and height coordinates and finally the transformation parameters for each image ID (ERDAS Imagine, u.d.). The data is referenced in SWEREF99 1800 (a zone of the transversal Mercator Projection used in SWEREF99 reference system). The resolution of the images is about 0.1m/pixel. The images were collected on August 28, 2014. 2014 was a hot year. In July and early August new heath records were registered and in July the heat and drought caused the biggest forest fire in Sweden since the 1950th. The second half of August was colder and massive rain falls dominated the study area. (SMHI, 2014)

3.2.2 OTHER DATA

The NNH point cloud was collected over the study area on May 7th 2011 using a LiDAR sensor. The point cloud is referenced in SWEREF99 TM. The data was initially collected by the Swedish surveying authority but was provided in this thesis from Metria. The following data was also provided by Metria:

- *TreeHeightRaster* – Raster containing registered heights for the forest in the area (Updated 2016).
- *Farmland* – Vector layer containing the registered farmland in the area stored as polygons.
- *Roads* - Vector layer containing the registered roads in the area.

4. SOFTWARE

The software used in this thesis are used for image matching, surface interpolation, analysis of results and visualization. This chapter will give a brief description of the software used, their background and origin, what they do and how they are used in this thesis.

4.1 IMAGE MATCHING SOFTWARE

4.1.1 KEYSTONE

Keystone is an image management system developed by Spacemetric. Spacemetric provides various services for satellite and airborne sensors. Keystone consists of several components; a server, a console and a web portal.

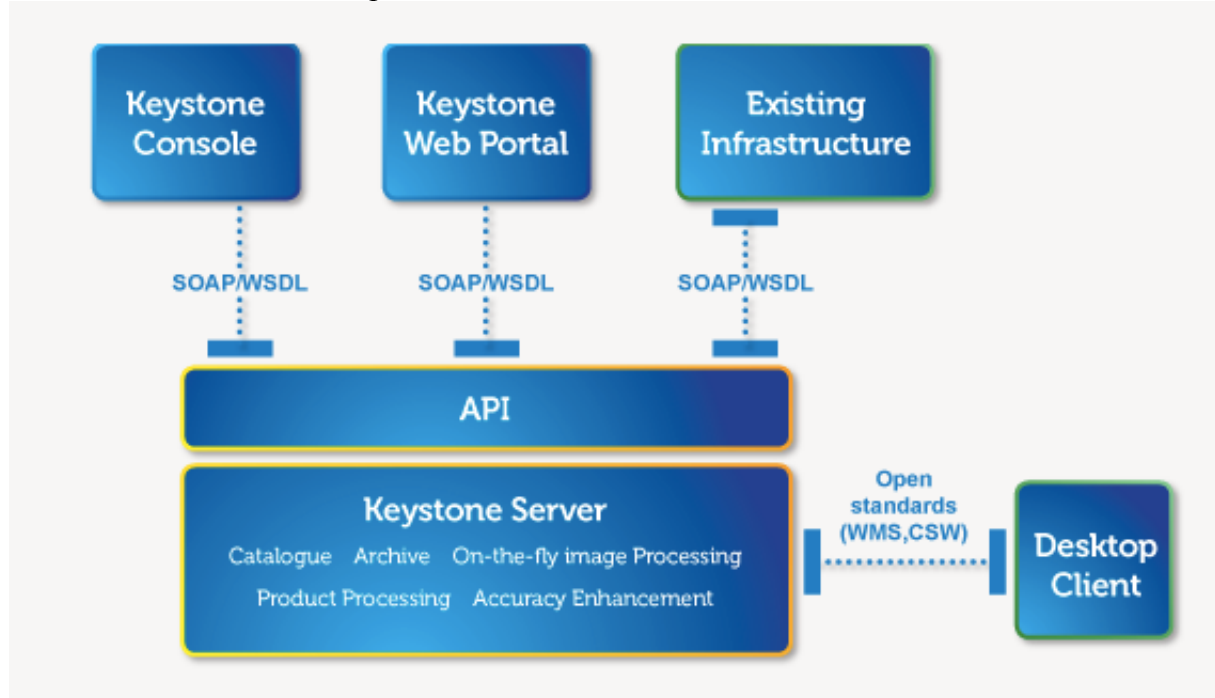


FIGURE 4. KEYSTONE COMPONENTS (SPACEMETRIC, 2016)

The server has a decentralized architecture allowing administrators to control the work flow and design, it can also be plugged in to existing infrastructure. The Keystone console allows the user to inter alia perform ortho-rectification, create outputs in over 3000 coordinate systems and visualize imagery with on-the-fly processing. The web portal works on any standard browser which enables access to Keystones core capabilities. (Spacemetric, 2016) In this thesis Keystone was solely used to photogrammetrically produce a point cloud from overlapping imagery. In order to import the imagery and their orientation a solo-standing small application was used. The application is not an official product but was produced for this purpose by Håkan Wiman, developer at Spacemetric Keystone.

4.1.2 ERDAS IMAGINE

ERDAS Imagine is a remote sensing application provided by Hexagon Geospatial. Hexagon geospatial is the GIS platform of Hexagon, a provider of information technologies (Hexagon geospatial, 2016). ERDAS imagine provides a varied range of analysis-, visualization- and data processing tools such as change detection tools, spatial modelling with raster, vectors and point cloud, user-friendly ribbon interface and support for optical panchromatic, multispectral and hyperspectral imagery, radar and LiDAR data (Hexagon Geospatial, 2015). ERDAS photogrammetry is included in the Producer suite of the Power Portfolio. ERDAS

photogrammetry uses state-of-the art photogrammetric satellite and aerial image processing algorithms. (Hexagon geospatial, 2016)

In this thesis ERDAS photogrammetry was used foremost to generate a point cloud from overlapping images. Furthermore, ERDAS Imagine was used to create differential images and to view results and set proper projections to the generated surfaces. ERDAS utilizes a Semi-Global Matching algorithm for point pair registration and allows few options for the user to affect the point cloud. The user can affect the strategies for how the images are matched by selecting the color band to match and set a threshold on the disparity difference allowed.

4.2 LASTOOLS

LASTools is the leading product of LiDAR processing tools produced by Rapidlasso GmbH. It offers a collection of tools including, classification, triangulate and clip tools just to name a few. A native GUI is available as well as a LiDAR processing toolbox for ArcGIS. The software can efficiently and fast process billions of LIDAR points into useful products. LASTools is partly open sourced, but for larger point data sets a license is required for full access and completes outputs. (Rapidlasso GmbH, 2016)

In this thesis LASTools was used to interpolate the point clouds into surfaces as well as compressing the LiDAR data into more manageable data files without losing important information. The compress tool is another product from Rapidlassos tool-set called *LASzip*, which compresses las-file formats into laz-file formats. This tool is completely open-source.

Three different interpolation techniques are used to generate the surfaces. *LAScanopy* interpolates the point cloud using percentiles, e.g. the 50th percentile will take the height of the 50th percentile in the given grid-cell. The grid cell size is an input that can be changed according to the users need. *LAScanopy* should be used on relative heights since it cuts out every point lower than 1.37 meters above ground for the reason that *LAScanopy* output should only contain vegetated areas. If the height is absolute, meaning it is related to an ellipsoid or geoid rather than the ground, this function will not work. In this thesis the height is absolute but all points are above 1.37 meters, resulting in all points being used and no filtering of lower vegetation is done. *LAScanopy* can generate all percentiles except for the 100th, to generate a surface made out by the highest point in every grid cell *LASgrid* is used. *LASgrid* calculates average, highest or lowest point height in every grid cell, highest being the 100th percentile.

4.3 ARCGIS

ArcGIS is a mapping software delivered by ERSI Inc. ArcGIS is wildly used across the globe and can perform visualization and cartography, geographical analysis, remote sensing analysis and much more. In this thesis ArcGIS is predominantly used for visualization of data as well as some processing. The tools used are: Clip, Zonal statistic, buffer and raster calculator. Clip is used to cut out a portion of a raster data set using a polygon as boundary. Zonal statistic calculates statistics of a raster within zones defined by polygons in another dataset. The buffer tool enlarges a polygon with a set distance value and the raster calculator is used to build map algebra expressions and applying them to raster datasets.

4.4 FUGROVIEWER

Fugroviewer is delivered by Fugro Geospatial. Fugroviewer allows the user to visualize data and perform simple analysis. It can view raster, vectors and LiDAR data in an easy way. The data can be viewed in 3D or profiles can be viewed and visualization colors and sizes can be changed. (Fugro Geospatial, 2016) In this thesis Fugroviewer was used to view and analyze point clouds generated by photogrammetry.

5. METHODOLOGY

This chapter describes the steps taken in this thesis. Figure 5 shows a flow chart of the basic steps that are explained further in chronological order in this chapter.

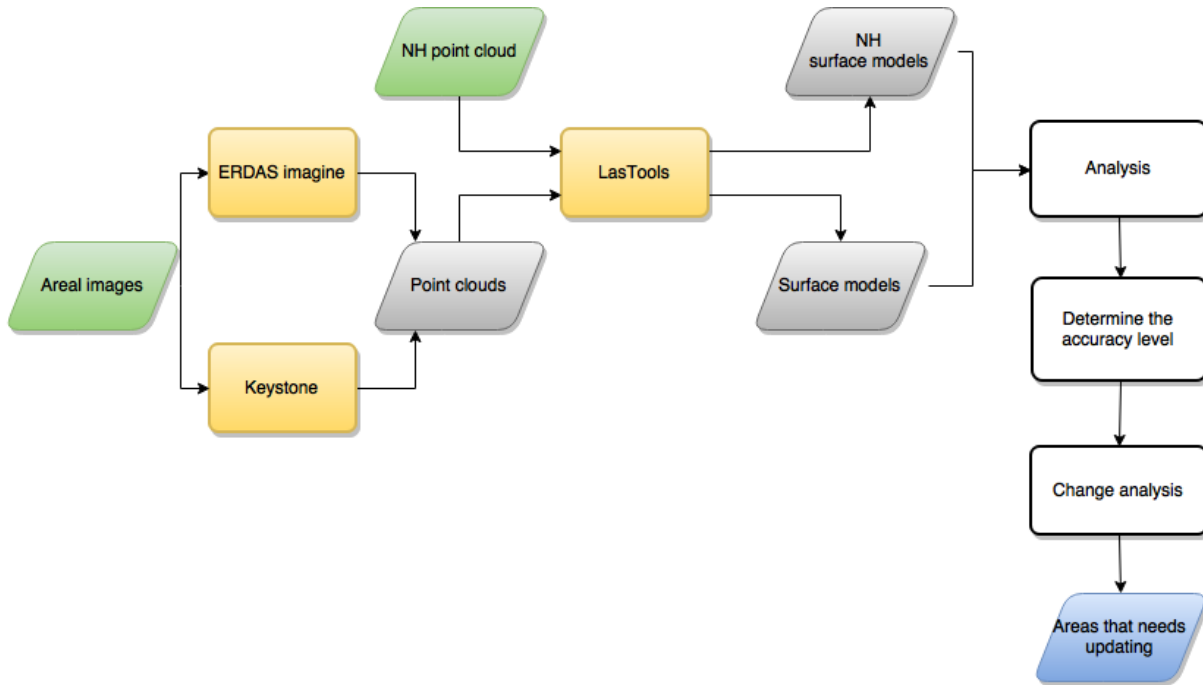


FIGURE 5. FLOWCHART OF THE METHODOLOGY

5.1 IMAGE MATCHING

5.1.1 KEYSTONE

A special extension was created for the purpose of importing the data into Keystone. The extension was built specially to import files with interior orientation given in ori-format. The extension also generates the point cloud, meaning that the Keystone console was only used to check the data and make sure nothing went wrong.

When importing the data, the directory to the images and the directory to the ori-file had to be set. For this to work it is important that the ID for each set of orientation parameters in the ori-file match the ID-name of the respective images. The coordinate reference system had to be named and the output-directory. The extension uses a Java-script to interpret the parameters and orient the images correctly.

Keystone, and the extension used in this thesis, allows the user to change almost all properties for the point cloud generation. The options include a choice of which spectral band to be used in the matching, a matching threshold, an edge threshold and a quality threshold. The matching threshold is the level of how well the points need to match in order to be accepted as a match. If the threshold is 0 a match needs to be perfect in order to be considered a match, if the threshold is 50 basically all matches are accepted and the point cloud will be dense and noisy. The Edge threshold affects which point pairs that should be accepted based on the texture and edge information, a low edge threshold value accept matches in areas with poor texture and a high value force rich texture in accepted matches. The quality threshold doesn't have any effect on the matching process but decides which of the points that are allowed into the point cloud. Every match gets a quality value between 0 and 100 based on the fit of the match in consideration to the surrounding pixels. In this thesis the settings recommended by the developer was used.

Another setting that needs to be set is the output size of the las-files. The size is determined as a geographical size. This feature allows the user to create output files that is manageable. In this thesis the output size for each las-file was 100*100 meter.

When importing the data every flight line (three different flight lines) was put in separate folders. When generating the point cloud this caused a problem. Between the flight lines “holes” were generated, some of the las-files contained a very small amount of points and visually appears to be empty. The developer, Håkan Wiman, performed tests and discovered that this can be solved by finding the areas where this occurred and then regenerate the point cloud just on these places. However, it was decided that this would not inflict any problems on this thesis, since the ‘holes’ simply carries the value ‘No Data’.

5.1.2 ERDAS IMAGINE

The imagery was imported to ERDAS Imagine Photogrammetry using the ‘*Import PATB Areal Triangulation Data*’ dialog. The dialog takes the orientation file, the reference system, average flying height and the interior orientation parameters including the focal length, pixel size and offsets. From this a block (.blk) file was created. The images were opened in the project and attached to the orientation information by the name of each photo being the ID-value in the ori-file. The orientation parameters are given in the direction of the flight direction and half the images were directed North-South and the other half the other way. Due to this the direction axis for each image had to manually be checked in the properties of the image and changed if it was wrong.

Once the images were properly imported in to the software the point cloud generation could start. The ‘*Automatic tie point measurement*’ tool was used to find tie points and ‘*Block triangulation*’ was used to estimate the exterior orientation parameters. Note that all orientations already exist, these steps are still necessary in order to perform the image matching. The steps basically confirm and use the information imported and prepares the data for image matching.

The ‘*XPro Semi-Global matching*’ was used for point cloud generation. The default settings were used in this thesis. That means that the green band was used for point pair matching and the disparity difference allowed was 1.

5.2 CREATE SURFACE MODEL

The point clouds were interpolated to surfaces using LAStools. Firstly, the operation LAS2LAZ was used in order to compress the data and therefore making it faster to store, copy and transmit between different folders. In order to handle inevitable outliers, several approaches were applied to the image matched point cloud.

5.2.1 IMAGE MATCHED SURFACE MODELS

As mentioned in chapter *National Height model (NNH)* the interpolated DEM generated from the NNH-point cloud have a resolution of 2 meters. Therefore, surfaces with a resolution of 2 meters were interpolated from the imaged matched point clouds as well. However, the motivation for this thesis is that by interpolating a point cloud that is expected to be contaminated by outliers it should be possible to exclude those outliers and achieve a higher accuracy than the point cloud itself. By interpolating the point cloud into surfaces with lower resolution every cell will include more points, hence more information that affect the surface. Using this reason, surfaces with resolutions of 5 meters and 10 meters were also created.

Furthermore, several interpolation techniques of the point clouds were implemented in order to try to exclude the outliers. The LAStools tools LAScanopy and LASgrid were used to interpolate the point clouds into surfaces using different percentiles. Percentiles is a way to chose a value from a set of values that are ordered according to their magnitude. Say you have

ten pixels with different height values attached to them, if you stack them on each other with respect to their height value so that the highest value ends up on top. The the 70th percentile would be the seventh highest pixel, the 30th percentile would be the third highest pixel and so on. The percentiles used in this thesis were the 50th, the 90th, the 95th and the 100th. The 50th percentile is the median of all points in the cell which is interesting due to the expected noise in the point clouds, the 100th is the highest hence it will include all positive outliers. The idea is that if there is a lot of noise the 50th percentile will work well in even out the noise, if the point cloud has a low noise but some random gross outliers then the 95th or 90th will exclude those.

5.2.2 NNH SURFACE MODELS

Since the NNH point cloud is used a reference that is assumed to be true there should not be any outliers. Of course there might be outliers, but this thesis will not gain from trying to exclude those. Since the point cloud is assumed to be true there is no need to use different interpolation techniques, hence only the 95th percentile was used to interpolate the NNH point cloud. The point cloud was interpolated into all three resolutions (2 meters, 5 meters and 10 meters) in order to be used as a reference and for comparison.

5.3 ANALYTICAL SUPPORT AND DETERMINATION OF ACCURACY LEVEL

5.3.1 FEATURE MASKS

It is expected to find great differences in the accuracy of points matched in areas with bare ground and in areas covered by forest. In order to separate the results of the two masks were created. The masks are bounding polygons that only include areas of interest. By intersecting or clipping the data with the mask the information of interest can be viewed without disturbance.

The mask for the bare ground (Figure 6) is extracted from the vector layer *Farmland* provided from Metria that maps fields registered for agricultural use. The layer is clipped to cover the study area. Fields, or bare ground, that is not registered for agricultural usage is therefore not included in the mask.

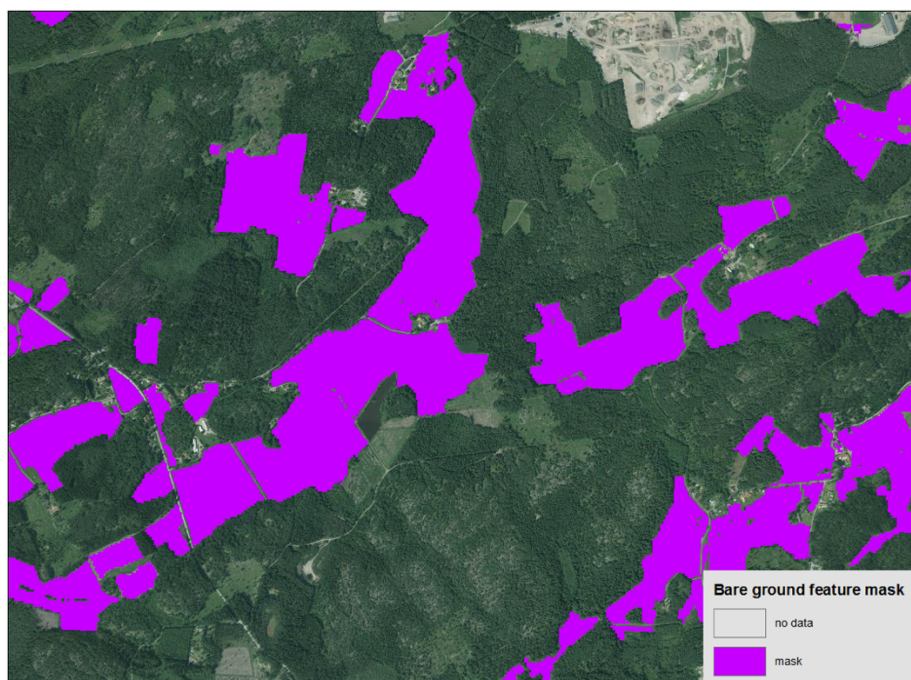


FIGURE 6. BARE GROUND FEATURE MASK

Since the growth of young forests varies in height it can be difficult to compare, hence only older forests are used as the mask for the forest (Figure 7). A Swedish coniferous forest typical for the study area region that has reached a height of 25 meters usually grows slowly. Deciduous forest on the other hand has a shorter life cycle and does not usually reach the same height as the coniferous forest. From the *TreeHeightRaster* data also provided by Metria, the pixels with a height of 25 meters or higher was used to mask older coniferous forest. The pixels were extracted using the *raster calculator* after the layer was clipped to fit the extent of the study area.

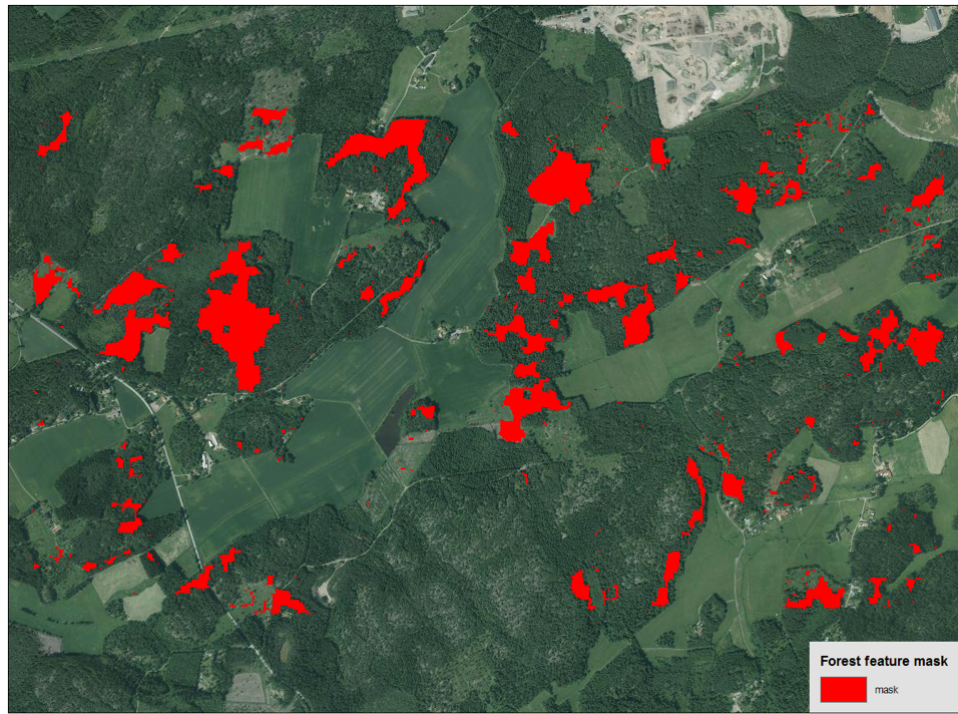


FIGURE 7. FOREST FEATURE MASK

5.3.2 SURFACE MODELS STATISTICS

In order to see how well the different resolutions and interpolation techniques affect the generated surface the difference between the surfaces and the image matched point cloud were compared through subtraction. All the surfaces generated from each image matched point cloud were subtracted with the image matched point cloud.

To do the comparison between a surface and a point cloud, the point cloud first had to be interpolated into a surface as well. The point cloud was interpolated with the 100th percentile and a resolution of 0.1 meter. The original aerial photos that were used for image matching had a resolution of 0.1 meters. By interpolating the point cloud into a surface with that same resolution there will be exactly one point or nothing in each cell, hence a perfect representation of the point cloud but in grid-format. Due to large data files, especially the representation of the point clouds, smaller representative areas were selected for each feature (bare ground and forest). The areas selected can be seen in Figure 8 and are 100*100 meters each, which is the output size of each point cloud file generated through Keystone. Through Keystone, polygons for the extent of each point cloud output-file was generated simultaneously as the point cloud, therefore those polygons were easily accessed and already in a manageable size. The two representative areas are two of those polygons. Difference images were created for each feature and all interpolations and resolutions. The output of the difference image has to be set to the highest resolution of the input layers, in this case 0.1

meters. If the resolution is set any lower than that, every point in the point cloud will not be compared to the surface.

The difference between the point cloud and and because of interpolation the interpolated surfaces should be zero if they match completely. However, due to noise in the point cloud they will not match perfectly hence other values were extracted in order to analyze the surfaces relative the point cloud. The values that might be interesting are the mean, the median and the mode. The mode value is the value most common in the data set, since the values are not rounded up or down the mode value in this case would be quite arbitrary. The value that is the most common might just occur a few times, therefore the mode value will not give any information of significance. The mean value includes all values in the data set, even the outliers and the median gives the middle value if all values was placed in order of their size. It can be expected that there will be gross outliers in the image matched point clouds, which would affect the mean value greatly therefore it was decided that the median value would be best to analyze the fit of the surfaces to the point cloud.



FIGURE 8. AREAS USED AS REPRESENTATION FOR THE FEATURES BARE GROUND AND FOREST.

5.3.3 SYSTEMATIC ERRORS

Systematic errors are errors that occur systematically, or continuously, in all images or results. The systematic errors that can occur in these surface include that the surface is constantly too low or too high with the same amount throughout the whole surface, or that the surface is constantly tilting throughout the whole surface. These systematic errors can occur due to faulty interior orientation of aerial images, wrong inputs in the image matching algorithm or due to initial data error. If a systematic error occurs for one of the surfaces from each image matching software point cloud then it is true for all surfaces from that software, hence the tests only needs to be carried out for one surface from each software.

Constant height error check

In order to see if a surface is constantly too high or low in comparison to the reference surface, ground truth data (GTD) extracted from the NNH point cloud is used. Since all vegetation is constantly changing the GTD needs to be extracted from areas without vegetation and that is known to not have changed in any other way between the times the data sets were collected. The data sets here are the aerial imagery used for photogrammetric extracted point clouds and the LiDAR data. In the study area there are roof tops and roads that fulfill the requirement of no change over time. Since rooftops are usually slanted they might be harder to compare than flat surfaces, therefore only roads are used. In the aerial imagery shadows from vegetation or buildings can disturb the photo matching, therefore the roads are trimmed down to only cover roads that are located in open areas and can not be disturbed by shadows. Furthermore, the roads are trimmed down to only cover the center of the roads in order to eliminate the risk of including pixels that only borders the roads but actually represents the field next to it. However, this problem can not be completely avoided since surfaces with a 10-meter resolution have pixels that are wider than the roads. The areas selected can be seen in Figure 9.

The difference images between the generated surfaces and NNH surface is intersected with the GTD areas using the *clip* tool in ArcGIS. Since the GTD only covers roads that have not changed, the mean value for the pixels in the difference image should be zero in those areas. If the mean is higher or lower, it can be assumed that a surface has a constant error. However, it can also be random errors. The statistics of the pixel values in the difference image also gives the standard deviation of the sample mean, see Equation 8. The standard deviation of the sample mean is calculated from the standard deviation in every pixel divided by the square root of the sample size(n). Equation 7 shows the standard deviation of one sample(every pixel) which is the mean height value(\bar{x}) in every pixel in the difference image and the deviation from that mean value(x_i) in every pixel(i). The sum of all deviations is divided by the sample size(n) minus 1 (Mattecentrum, 2016).

$$\sigma_i = \sqrt{\frac{\sum(\bar{x}-x_i)^2}{n-1}} \quad (7)$$

$$\sigma = \frac{\sigma_i}{\sqrt{n}} \quad (8)$$

If the standard deviation multiplied by two (95%-confidence interval) is larger than the mean, it is assumed to be within the expected random error and no constant height error can be determined.

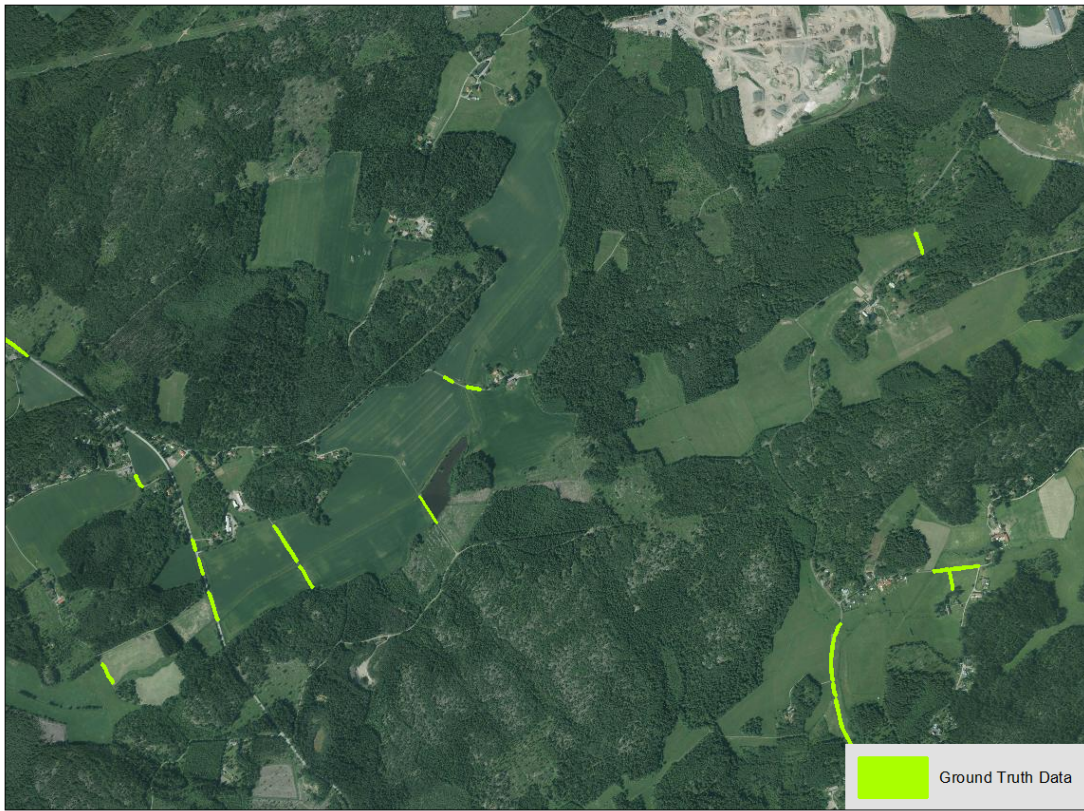


FIGURE 9. GROUND TRUTH DATA

Tilt check

A tilt-check was carried out in order to detect if the surfaces were continuously tilting over the study area. To see if the area is tilting polygons distributed across the study area is needed. In this case the bare ground mask created in chapter 5.3.1 *Feature masks* was used. The mask contains polygons of areas registered as agricultural land, as seen they are distributed across the study area. These polygons were intersected with a difference image using *zonal statistics* in ArcGIS (Esri, 2011). *Zonal statistic* calculates a statistical value from the raster layer for each zone in the zone layer. The statistical value that was calculated here was the mean. This operation generates a shape file containing the polygons with the mean value of all pixels that the polygons intersect. If there is any tilting this will be visible since the mean values of the polygons will change continuously throughout the study area.

5.4 CHANGE DETECTION

Change detection images were created by subtracting the image matched-surfaces from the NNH-generated surfaces. A threshold for the extent of change that can be detected was applied with regards to the result from the systematic height error check.

The threshold was set according to the standard deviation for each surface in relation to the NNNH-surface. Everything within the threshold of two times the standard deviation is considered as no change, or undetectable change. Everything above is considered as growth and everything under is considered negative change, meaning something has been taken down. Everything under -20 is considered deforestation. The reason for this is that trees taller than 20 meters are usually the target for financial deforestation and therefore should be easier to pin point and is interesting to find. These thresholds are considered classes in this thesis.

The classes were created by using the spatial modeler in ERDAS Imagine and different ranges were given a new value. The newly classified raster was grouped using *clump* in ERDAS (hexagongeospatial, 2015). *Clump* identifies continuous groups of pixels in one thematic

class. The output is an image-file containing the x and y coordinates for each clump. The clumps, or groups, of pixels are assembled by neighboring pixels with the same class. The neighbors can be defined either as four completely connected neighbors or eight connected neighbors see Figure 10 for illustration of four or eight neighbors. In this thesis four neighbors were used, this means that the requirement for a neighbor is restricted to have a full side of the pixel lining with a full side of the neighboring pixel. If eight neighbors would have been chosen, more pixels would be accepted as part of a neighborhood and the smoothening of the surface would be less eminent.

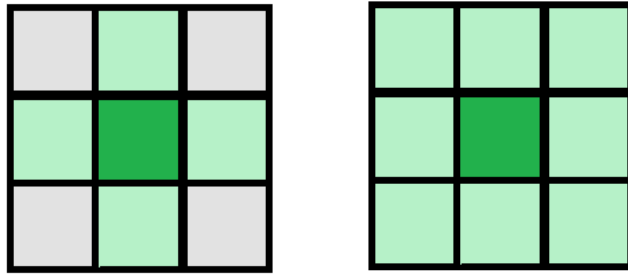


FIGURE 10. NEIGHBOR DEFINITION FOR THE ERDAS CLUMP FUNCTION. FOUR AND EIGHTH NEIGHBORS RESPECTIVELY

The image file containing grouped (clumped) pixels was then put through another ERDAS function called *Eliminate* (hexagongeospatial, 2015). *Eliminate* counts the pixels in each group (clump) and only keeps those groups that contain an equal or larger amount of pixels than a set threshold. The groups that contain a smaller amount of pixels than the set threshold are dissolved to the neighbor groups value. The change detections shown in the result used a threshold of 20 pixels. By eliminating pixels that aren't grouped with other pixels in the same class of change, outliers are avoided.

5.5 NOISE REDUCTION AND ELIMINATION OF GROSS ERROR

Noise reduction and elimination of gross errors was not initially performed on either the point cloud or any of the surfaces. When evaluating the results, it dawned on the author that eliminating gross errors might efficiently enhance the accuracy of the forest feature of the image matched surfaces. Therefore, noise reduction and elimination of gross errors was performed on one of the surfaces in order to test this hypothesis. The result of this test is given in 6.2.4 *Noise reduced surface*. To find the noise and gross errors the reference surface(NNH) was compared with the surface that was tested. The reference surface was subtracted by the surface that was tested and statistics explained in 5.3.2 *Surface models statistics* was used. The Gross errors were considered any height value that exceeded the value of three times the standard deviation(3σ). The values that were considered gross errors were eliminated using the model builder in ERDAS Imagine. The model builder filtered the difference image and overwrote any pixel with a height value exceeding $\pm 3\sigma$ as 'NoData'. The standard deviation (σ) calculated for each photogrammetric surface is dependent on the quality of the reference surface and it is unique for each photogrammetric surface. Therefore, the standard deviation must be uniquely calculated for each surface that is tested and the 3σ -value calculated in this thesis can not be reused.

6. RESULT AND ANALYSIS

In this chapter the point clouds and surfaces will be presented both in 3D-images, statistical results and written observations. First the photogrammetric point clouds will be presented, first visually where profile views and overviews are displayed, then the point clouds accuracy in relation to the NNH-point cloud is presented. The second part views the generated surfaces. A visual overview is given, with visual comparison to the NNH-point cloud. The result from the systematic error check is shown and a comparison between the generated surfaces and their respective photogrammetric point cloud the are generated from is presented. Finally, an accuracy estimation of the surfaces is given. The final part of this chapter includes the change detection, where the different steps in producing a change detection image is shown.

6.1 IMAGE MATCHED POINT CLOUDS

Two point clouds were generated in this thesis. The first point cloud is from ERDAS imagine and the second point cloud is from Keystone. Here those point cloud are presented and compared to the NNH-point cloud. They are not compared to each other since it is not part of the thesis but their similarities confirm that the result in this thesis is not based on a point cloud generated from an inferior matching algorithm. If the point clouds would have been a lot different, it would have been necessary to investigate the image matching algorithm to see which one represents the ability of image matching algorithms today.

6.1.1 KEYSTONE

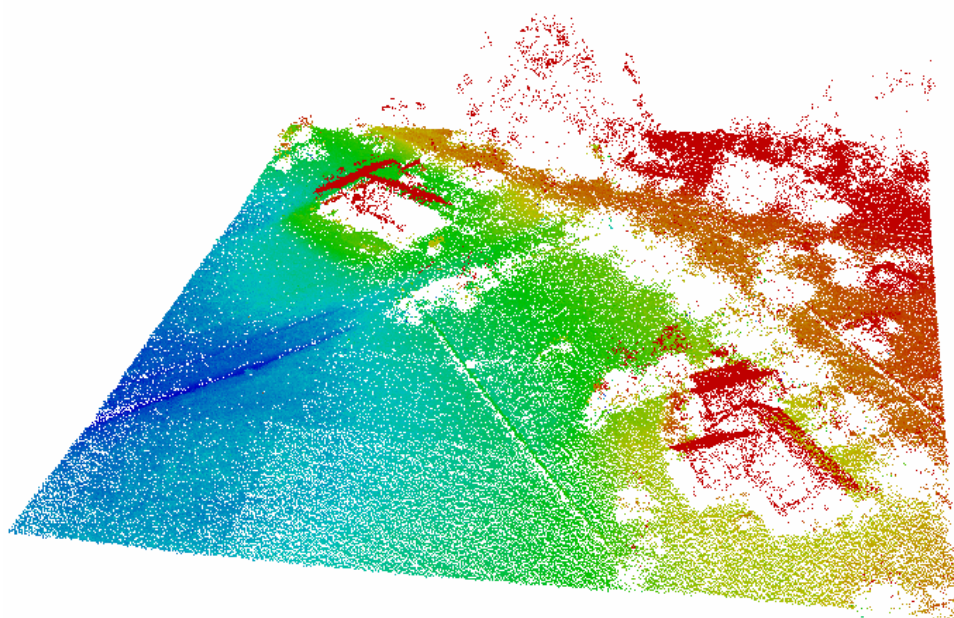


FIGURE 11. 3D VIEW OF A POINT CLOUD-TILE FROM KEYSTONE SHOWING TWO HOUSES AND SPARSE FOREST. POINTS ARE COLORED BY ELEVATION.

In Figure 11 a snip of the generated point cloud from Keystone is shown. Houses can be seen clearly and trees are captured. Even a road in the far left in Figure 11 can be distinguished as well as what looks like ditches around the house. The point cloud is dense and when colored by elevation it is easy to see different features. It can be seen that under trees and houses there are no points and that the façades of the houses are not in the point cloud.

Figure 12 shows Keystones point cloud and NHH point cloud. The Keystone point cloud is shown in red and NNH point cloud is shown in green.

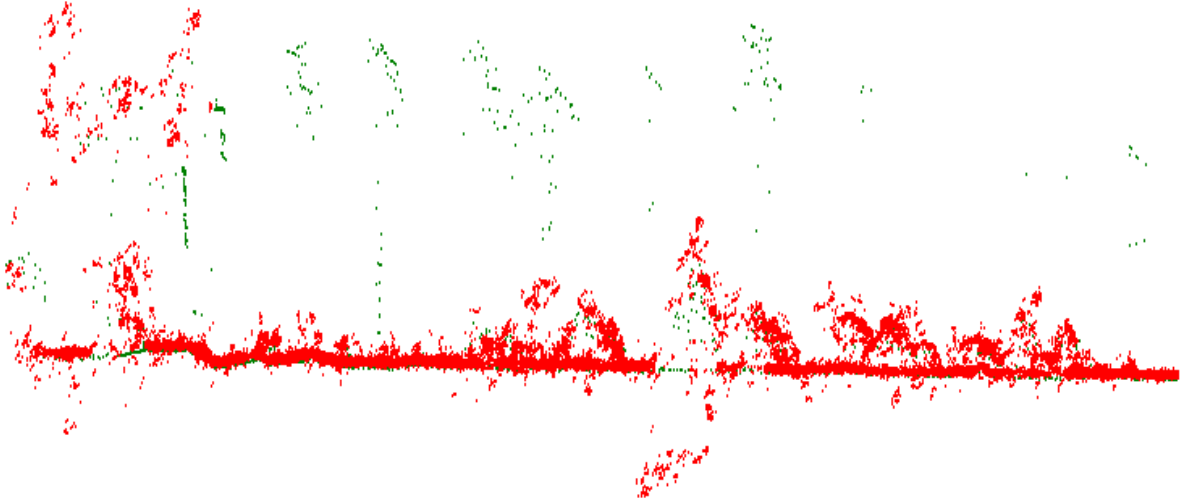


FIGURE 12. PROFILE VIEW OF DECIDUOUS AND CONIFEROUS FOREST. NNH POINT CLOUD SHOWN IN GREEN AND KEYSTONE POINT CLOUD SHOWN IN RED

The NNH point cloud includes points in the trees but not the point cloud generated from image matching with Keystone. Smaller trees, probably coniferous trees, is included in the Keystone point cloud. Where there are high trees included in the NNH point cloud the Keystone point cloud only include low vegetation and bare ground. There is a lot of noise in the Keystone point cloud, probably due to the confusion with the coniferous trees and some of the confusion seems to have generated gross outliers. When the point pairs are faulty matched the trigonometric calculations (*2.1 Stereo-photogrammetry*) gets skewed and gross outliers occur.

6.1.2 ERDAS IMAGINE

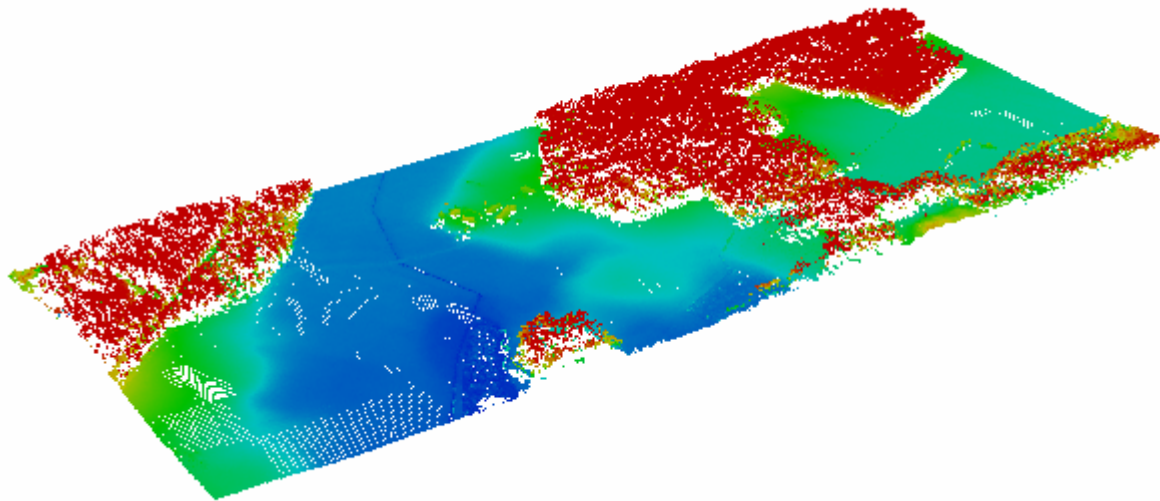


FIGURE 13. 3D-VIEW OF ONE POINT CLOUD-TILE GENERATED THROUGH ERDAS SHOWING BARE GROUND AND FOREST. POINTS COLORED BY ELEVATION.

In Figure 13 a part of the point cloud generated from ERDAS image matching is shown. The visualization has rendering errors in the left bottom corner, which is due to the graphic card in the computer used and not something that has to do with the point cloud. The point cloud appears to be dense and in the middle a ditch in between the fields can be seen. Forest features are clearly visible and the slope in the fields is visible as well.

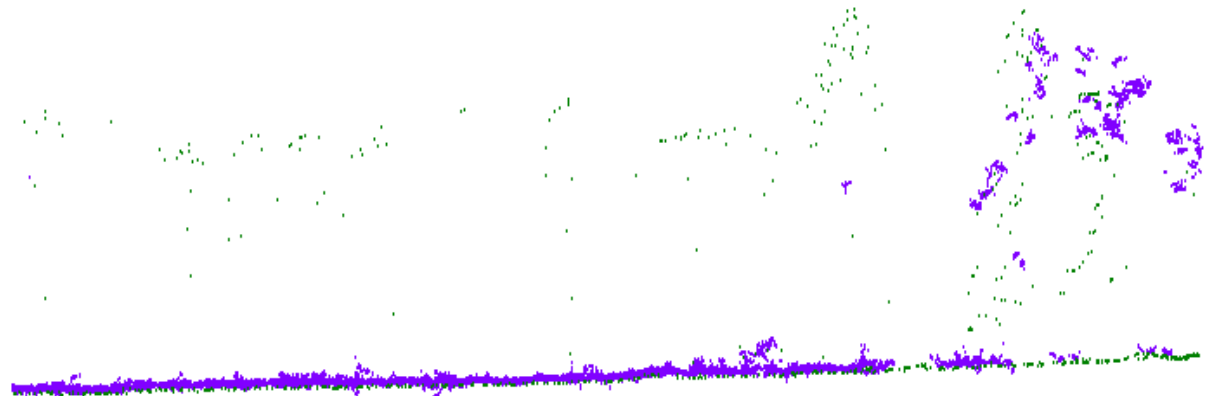


FIGURE 14. CONIFEROUS AND DECIDUOUS FOREST. NNH POINT CLOUD SHOWN IN GREEN AND ERDAS POINT CLOUD SHOWN IN PURPLE

Figure 14 show the same area as in Figure 12. The point cloud from ERDAS, just like the point cloud from Keystone, does not register the deciduous trees that is registered in the NNH point cloud. The distribution of the points is a bit scattered but no gross outliers can be seen in this profile view. In the right of the image are coniferous trees that ERDAS has registered.

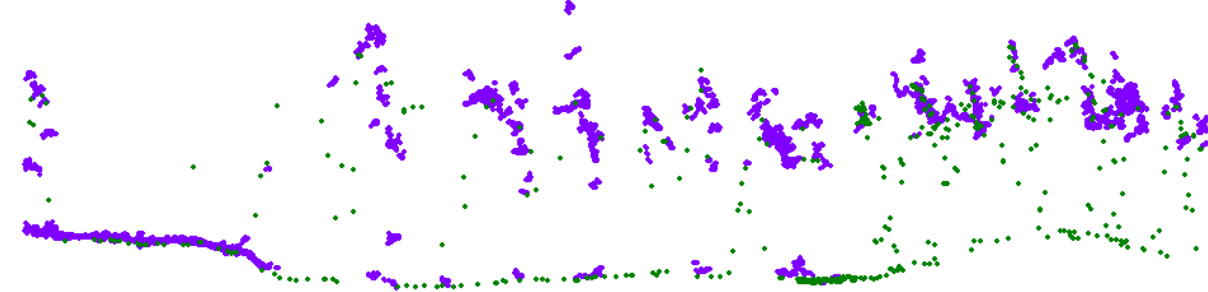


FIGURE 15. BARE GROUND AND CONIFEROUS FOREST, NNH POINT CLOUD SHOWN IN GREEN AND ERDAS POINT CLOUD SHOWN IN PURPLE

Figure 15 shows an area with coniferous forest. The ERDAS point cloud follows the tree profile well but does not catch points in between the trees or the ground in between in areas with dense forest. Points between some trees are registered. In the left side of the image there is bare ground. It can be seen that the ERDAS point cloud has more noise than the NNH point cloud and that it appears to be located a bit higher.

6.1.3 POINT CLOUD ACCURACY

TABLE 1. ACCURACY OF GENERATED POINT CLOUDS IN RELATION TO THE NNH-POINT CLOUD

<i>Values in meter</i>		Mean value	σ	2σ
ERDAS	Bare ground	0,30	0,035	0,07
	Forest	3,20	7,099	14,198
Keystone	Bare ground	0,36	0,062	0,124
	Forest	3,34	6,999	13,998

Table 1 shows the mean value and standard deviation(σ) of the difference between the photogrammetric generated point cloud and the reference NNH point cloud. The areas used for the bare ground and forest feature can be seen in Figure 8.

Referring to the 95%-confidence interval(5.3.3 Systematic errors), everything within the range of 2σ is considered as non-detectable change and the values outside of the range are differences that can be measured. This shows how well the photogrammetric point cloud correspond to the reference point cloud(NNH), here referred to as the accuracy of the photogrammetric point cloud. It can be seen that no difference can be detected for the forest feature but significant difference can be found for the bare ground feature in both the photogrammetric point clouds. This difference is likely to be a result of vegetation growth in the fields since the acquisition dates of the two data sets compared are months apart. Since both the Keystone and ERDAS point clouds show a mean value above zero, it can be assumed that the fields have grown during the summer. It can also be seen that the accuracy for the forest feature for both Keystone and ERDAS is remarkably worse than for the bare ground feature.

6.2 IMAGE MATCHED SURFACE MODELS

In this chapter the image matched surfaces are presented and evaluated on how well they follow their origin point cloud they were interpolated from. The analysis is divided into the two different features, bare ground and forest.

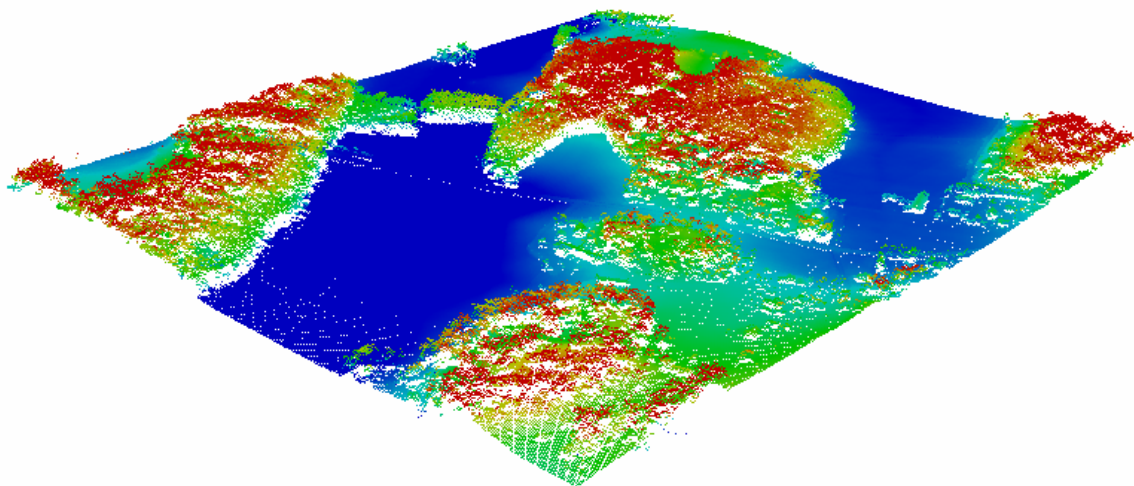


FIGURE 16. 3D-VIEW OF SUBSECTION OF INTERPOLATED SURFACE KEYSTONE WITH PERCENTILE 50(P50) AND 2-METER RESOLUTION, THE POINT CLOUD IS COLORED BY ELEVATION

In Figure 16 a surface of the 50th percentile and with a resolution of 2 meters is shown. The Points are colored by elevation and it is easy to distinguish the different features. Forest features of different height are well reproduced and bare ground can be seen both as fields and as hillier ground around houses. Houses can be seen in the right corner and even some roads are distinguishable.

6.2.1 FIT TO THE SOURCE POINT CLOUD

Bare ground feature

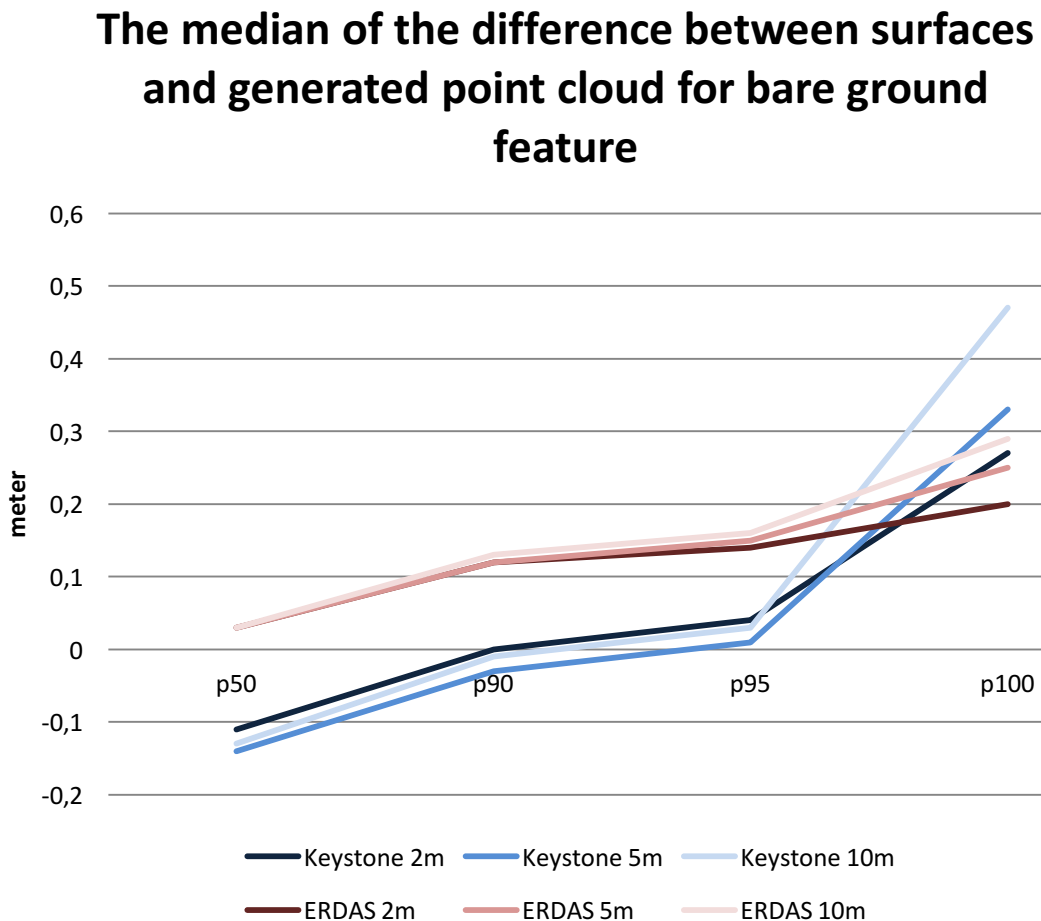


CHART 1. MEDIAN VALUE FOR DIFFERENCE IMAGE BETWEEN IMAGE MATCHED SURFACES AND IMAGE MATCHED POINT CLOUD FOR BARE GROUND FEATURE

In Chart 1 the bare ground feature doesn't show much variation between the different interpolation percentiles. The biggest variation is between 100th percentile and the rest. The surfaces with 10-meter resolution seem to be the most affected by the outliers since it increases the most with the 100th percentile. The surfaces with 2-meter resolution have the smallest variation of value between the interpolation percentiles since the line has flatter slopes. The ERDAS surfaces and the Keystone surfaces don't follow the same pattern, indicating there are differences between the point clouds. The surfaces generated from the ERDAS point cloud has an increasing change in value between the interpolation percentiles. When interpolated with the 50th percentile the resolution have a low effect on the result, higher percentiles are more affected by the increasing resolution. Furthermore, best fit of the Keystone point cloud seems to be interpolations with the 90th or 95th percentiles and for the ERDAS point cloud the 50th percentile.

Forest feature

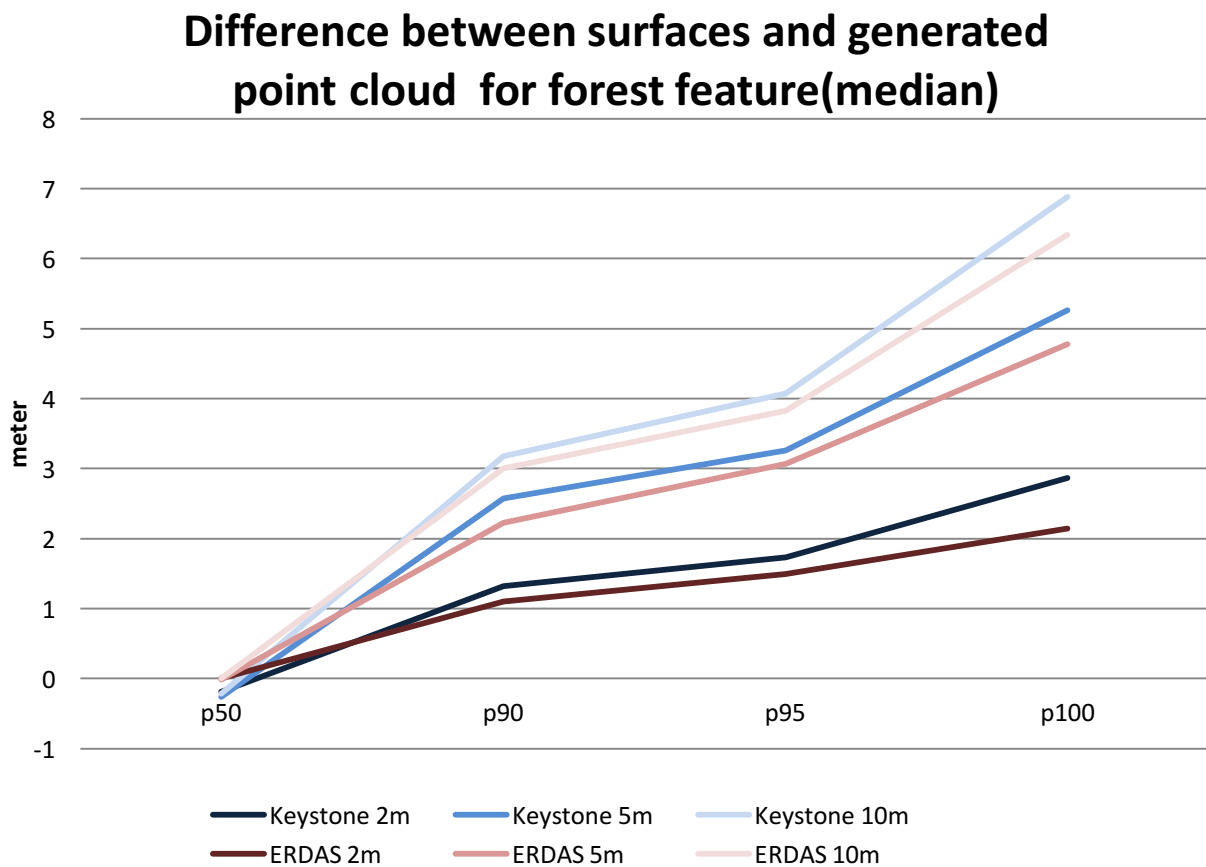


CHART 2. MEDIAN VALUE FOR DIFFERENCE IMAGE BETWEEN IMAGE MATCHED SURFACES AND IMAGE MATCHED POINT CLOUD FOR FOREST FEATURE

In Chart 2 the median value of the differential image between the point cloud and the interpolated surfaces are shown for the forest feature. The values are much higher than for the bare ground feature, for the forest feature the differences are on the meter scale. Since the forest features naturally have a higher variation than the bare ground feature, and error sources such as shadows between the tree tops exist the comparison between the point cloud and the surface will show a higher diversion in the forest feature. Most values are also positive, meaning the surfaces in general are higher than the point cloud.

The variation between the different resolutions are evident, the difference between the resolutions increases with the different percentiles. Similar to Chart 1 the lowest resolution is affected the least by the different resolutions. The best fit of the point cloud is generated by the 50th percentile.

Effect of different percentiles and image resolutions



FIGURE 17. PROFILE VIEW OF SURFACES INTERPOLATED FROM KEYSTONE POINT CLOUD. KEYSTONE POINT CLOUD IS SHOWN IN GREY. THE DIFFERENT PERCENTILES ARE SHOWN AS FOLLOWING; 50TH PERCENTILE SHOWN IN TURQUOISE, 90TH PERCENTILE SHOWN IN GREEN, 95TH PERCENTILE SHOWN IN RED

In Figure 17 different interpolation percentiles are shown together with the source point cloud. The 50th percentile captures more of the lower areas of the trees and the ground while the higher percentiles capture the tree tops. The 100th percentile follows the highest points in the point cloud and create a surface that looks like a blanket being put on top of the trees. The 90th and 95th percentiles follow the tree tops but are lower between the trees, causing the surface to be more variant.

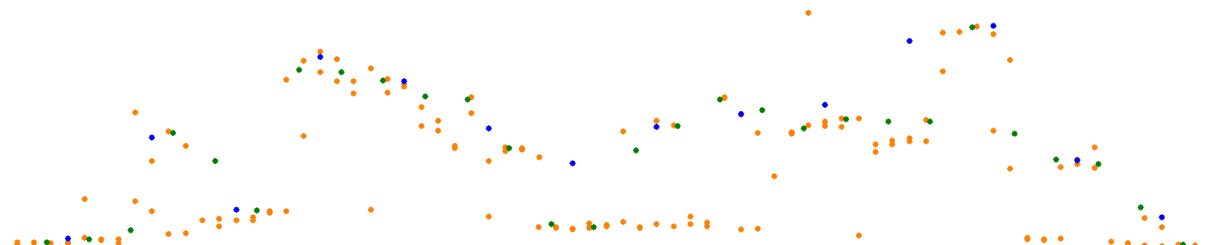


FIGURE 18. PROFILE VIEW OF SURFACES INTERPOLATED FROM ERDAS POINT CLOUD. 2-METER RESOLUTION SHOWN IN ORANGE, 5 METER RESOLUTION SHOWN IN GREEN AND 10 METER RESOLUTION SHOWN IN TURQUOISE

Figure 18 shows how different resolutions affect the interpolated surfaces. A higher resolution follows the profile while a lower resolution evens out the edges. As shown in *Chart 2* a surface with a resolution of 10 meter will have a higher median value than a surface with a higher resolution. This was seen in *chart 2* as the difference median of the interpolated surface subtracted by the point cloud being higher for surfaces with lower resolution. In opposite to that a lower resolution evens out edges a higher resolution keeps the variations in the point cloud and shows areas between trees.

6.2.2 SYSTEMATIC ERROR

Tilt -check

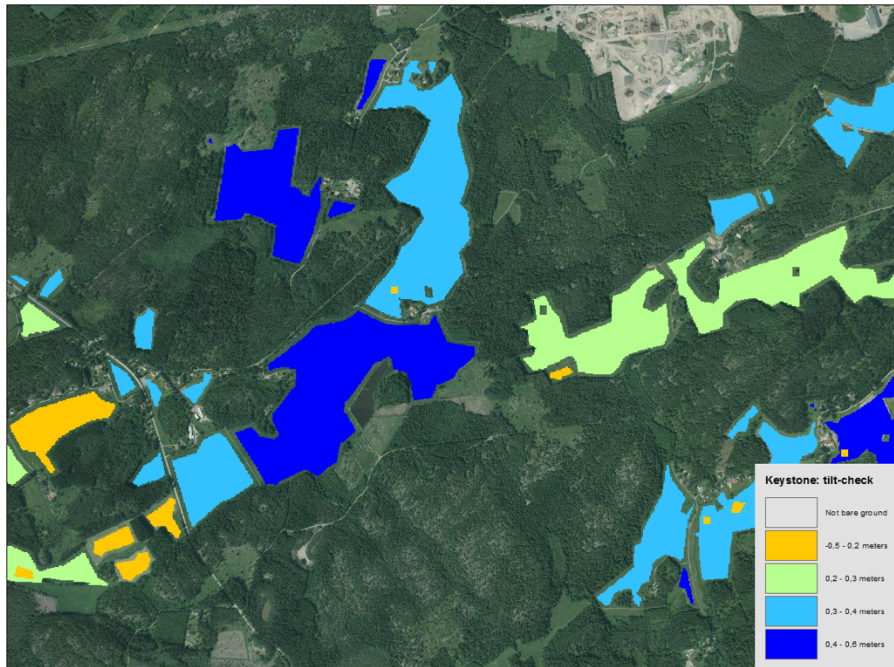


FIGURE 19. TILT-CHECK FOR KEYSTONE SURFACE, LEGEND SHOW DIFFERENCE IN HEIGHT VALUE FOR EACH POLYGON

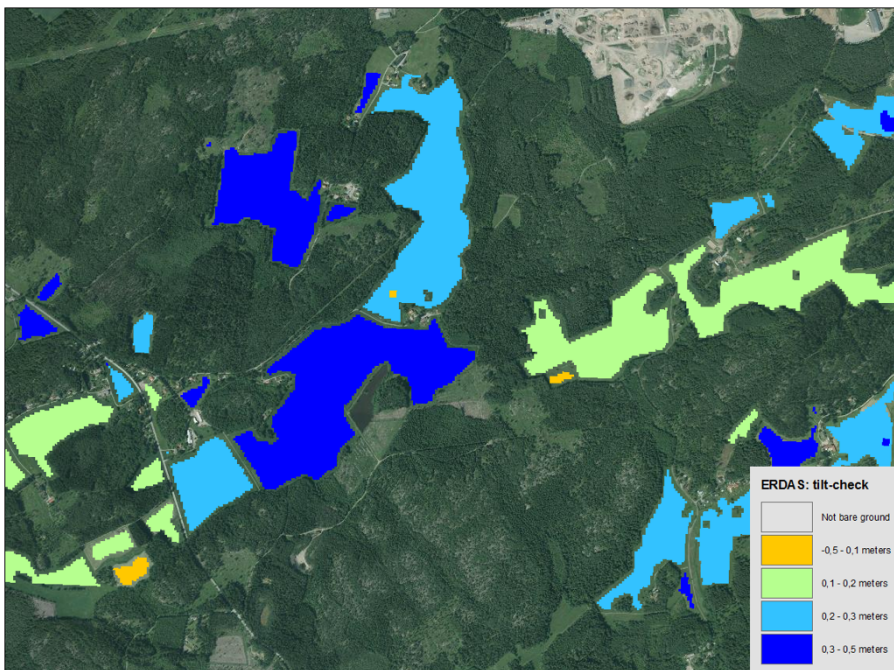


FIGURE 20. TILT-CHECK FOR ERDAS SURFACE, LEGEND SHOW DIFFERENCE IN HEIGHT VALUE FOR EACH POLYGON

In Figure 19 and Figure 20 the result from the tilt-checks are shown. The surfaces with bare ground feature would have shown a continuous change in height for each polygon from one side of the study is to the other if the surface would have been tilted. No such continuous pattern is found in either of the surfaces. Both surfaces show that the fields in slightly to the left of the center in the study are generally higher than the far left of the study area.

Continuous height error

TABLE 2. DIFFERENCE VALUES BETWEEN GENERATED SURFACES AND INTERPOLATED (WITH P95) SURFACE OF NNH POINT CLOUD IN GTD AREAS(FIGURE 9).

Values in meters		Max	Min	Mean	σ	2σ
Keystone						
2m	p50	0,59	-4,94	0,15	0,28	0,56
	p90	4,82	-4,78	0,39	0,32	0,64
	p95	6,1	-4,73	0,47	0,35	0,7
	p100	12,09	-4,26	0,96	0,81	1,62
5m	p50	0,34	-10,41	-0,13	0,96	1,92
	p90	1,21	-9,73	0,16	0,95	1,9
	p95	1,38	-9,12	0,25	0,93	1,86
	p100	10,44	-7,81	1,28	1,52	3,04
10m	p50	0,63	-12,81	-0,51	1,94	3,88
	p90	1,22	-12,49	-0,14	1,93	3,86
	p95	1,3	-12,4	-0,04	1,92	3,84
	p100	12,03	-6,47	1,75	2,65	5,3
ERDAS						
2m	p50	0,63	-4,95	0,15	0,27	0,54
	p90	0,8	-4,83	0,26	0,28	0,56
	p95	2,1	-4,8	0,28	0,28	0,56
	p100	8,88	-4,60	0,35	0,39	0,78
5m	p50	0,38	-12,12	-0,14	1,21	2,42
	p90	0,64	-11,57	0,03	1,17	2,34
	p95	0,85	-9,13	0,08	1,03	2,06
	p100	5,1	-7,3	0,33	0,8	1,6
10m	p50	0,28	-11,71	-0,46	1,66	3,32
	p90	0,66	-11,19	-0,18	1,59	3,18
	p95	0,89	-10,93	-0,1	1,5	3
	p100	9,1	-6,64	0,44	1,45	2,9

Table 2 shows statistic from the difference between the photogrammetric generated surfaces and the surface interpolated from the NNH point cloud with the 95th percentile. The values are only extracted from areas included in *Figure 9. Ground truth data*, hence areas where no change definitely should not have occurred. If a surface is continuously too high or low (systematic error), the mean value will not be zero. However, certain random errors are expected. The values are accepted to be normally distributed and values within +/- 2 σ are, with a 95 percent confidence level, random errors. Since the mean value for all surfaces are within the respective interval they are considered to be, with a confidence of 95%, within the range of random variations hence no constant height error is detected.

Since values within +/- 2 σ are considered random variations, changes within that range can not be found. It can also be said that changes that are found and that does not fall in that range of +/- 2 σ have an accuracy of +/- 2 σ .

The narrowest range of random variations can be seen in the 2-meter resolution, while 10-meter resolution generates the widest range of random variations. For the Keystone surfaces interpolations with the 100th percentile give a wider range of random variation than the other

percentiles hence smaller changes can be found in surfaces interpolated with other percentiles. For the ERDAS surfaces the two higher resolutions have a narrower range of random variation.

6.2.3 SURFACE ACCURACY ASSESSMENT

This chapter presents the accuracy of the surfaces in relation to the reference point cloud, the NNH point cloud. The accuracy is again divided into the two features forest and bare ground. First a diagram showing the median of the difference between NNH and the image matched surfaces, then a table of the fit is given showing the accuracy of for each feature.

Median of bare ground feature for difference image between NNH and image matched surfaces

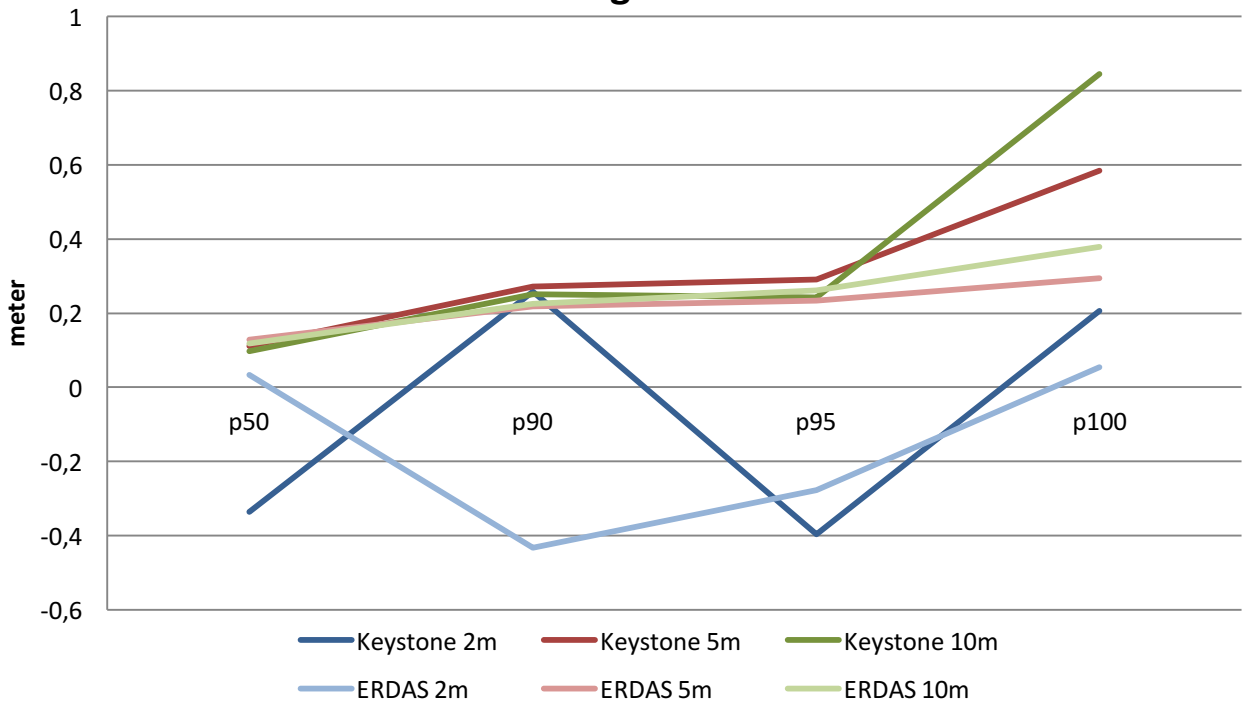


CHART 3. MEDIAN FOR DIFFERENTIAL IMAGES OF BARE GROUND FEATURE

In chart 3 the median of the bare ground feature for the difference image between images matched surfaces and NNH point cloud is shown. The surfaces with a resolution of 5 and 10 meters follow similar patterns, for the 50th percentile the values are similar and the variation between them increases with higher interpolation percentiles. The lines for the surfaces with a resolution of 2 meter varies a lot, however the y-axis is on a decimeter scale which means that the variations are not that big. According to Chart 3 the 100th percentile for the 5- and 10-meter resolution show a positive change and the 2-meter resolution show either no difference or a negative change. A lot of the values falls within the range of their respective $\pm 2\sigma$, which means that the change might as well be due to random variation.

TABLE 3. ACCURACY OF IMAGE MATCHED SURFACES IN REALTION TO NNH POINT CLOUD FOR BARE GROUND FEATURE (VALUES IN METER)

Accuracy for bare ground feature (ERDAS)				Accuracy for bare ground feature (Keystone)			
	Mean value	σ	2σ		Mean value	σ	2σ
2m				2m			
50th	0,18	0,44	0,88	50th	0,17	0,45	0,9
90th	0,25	0,44	0,88	90th	0,32	0,49	0,98
95th	0,27	0,44	0,88	95th	0,36	0,55	1,1
100th	0,18	0,44	0,88	100th	0,673	1,04	2,08
5m				5m			
50th	0,12	0,21	0,42	50th	0,14	0,22	0,44
90th	0,21	0,2	0,4	90th	0,3	0,24	0,48
95th	0,24	0,2	0,4	95th	0,35	0,36	0,72
100th	0,34	0,23	0,46	100th	1,02	1,68	3,36
10m				10m			
50th	0,09	0,24	0,48	50th	0,05	0,26	0,52
90th	0,23	0,23	0,46	90th	0,24	0,27	0,54
95th	0,26	0,23	0,46	95th	0,29	0,34	0,68
100th	0,42	0,31	0,62	100th	1,65	2,55	5,1

Median of forest feature for difference image between NNH and image matched surfaces

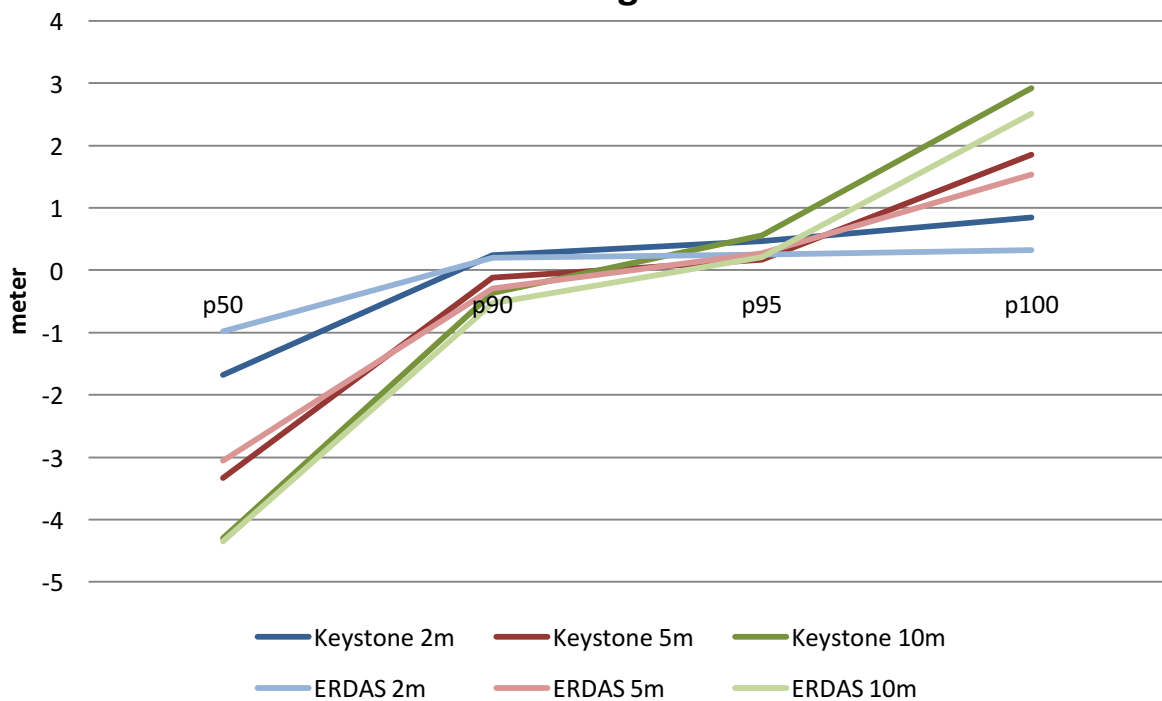


CHART 4. MEDIAN FOR DIFFERENTIAL IMAGE OF FOREST FEATURE

In Chart 4 the median of the forest feature for the difference image between images matched surfaces and NNH point cloud is shown. The difference detected is larger than for the bare ground feature (Chart 3). All three resolutions follow roughly the same pattern over the interpolation percentiles. The surfaces with a resolution of two meter vary the least from zero, while the surfaces with a resolution of 10 meters varies the most hence more difference is found in the lower resolutions.

It can be seen that the 90th and 95th percentiles gives median values closer to zero than the 50th and 100th percentiles. All values for the 95th percentile are positive while the values for the 90th percentile are both positive and negative. The median value grows in size with the percentiles, this makes sense since it's the difference of the interpolated surfaces and the NNH point cloud and the 100th percentile will naturally have a higher value than the lower percentiles.

TABLE 4. ACCURACY OF IMAGE MATCHED SURFACES IN REALTION TO NNH POINT CLOUD FOR FOREST FEATURE (VALUES IN METER)

Accuracy for forest feature (ERDAS)				Accuracy for forest feature (Keystone)				
	Mean value	σ	2σ		Mean value	σ	2σ	
2m	50th	-1,71	7,79	15,58	50th	-1,35	8,02	16,04
	90th	0,45	7,4	14,8	90th	0,92	7,7	15,4
	95th	0,86	7,36	14,72	95th	1,4	7,66	15,32
	100th	-1,76	7,78	15,56	100th	2,37	7,59	15,18
5m	50th	-4,89	6,96	13,92	50th	-5,03	7,06	14,12
	90th	-0,98	6,2	12,4	90th	-1,39	6,67	13,34
	95th	-0,04	6,02	12,04	95th	-0,53	6,53	13,06
	100th	1,72	5,77	11,54	100th	1,88	6,15	12,3
10m	50th	-6,93	6,95	13,9	50th	-6,62	7,1	14,2
	90th	-1,9	5,8	11,6	90th	-1,91	6,37	12,74
	95th	-0,65	5,41	10,82	95th	-0,75	6,17	12,34
	100th	2,52	4,56	9,12	100th	2,57	5,25	10,5

6.2.4 NOISE REDUCED SURFACE

Here the accuracy of the noise reduced and gross error eliminated surfaces is given. This result was generated late in the process of this thesis. Therefore, the result only covers the surfaces of different resolutions for the 100th percentile from the Keystone point cloud. The comparison is, like in Table 3 and Table 4, in relation to the NNH point cloud.

TABLE 5. ACCURACY FOR NOISE REDUCED SURFACES OF FOREST FEATURE INTERPOLATED WITH THE 100TH PERCENTILE FROM KEYSTONE POINT CLOUD

Accuracy for noise reduced forest feature (Keystone, 100 th percentile)			
Values in meter	Mean value	σ	2σ
2 meter	1,907	4,201	8,402
5 meter	2,296	3,756	7,512
10 meter	3,045	3,21	6,42

Table 5 shows the values for two time the standard deviation (2σ) i.e. the accuracy of the surface feature. The noise reduced surface has a significantly better accuracy than the non-noise reduced surface given in Table 4. The difference is almost double in the non-noise reduced surface. It can also be seen that a higher resolution gives better accuracy in the noise reduced surface too.

6.3 CHANGE DETECTION

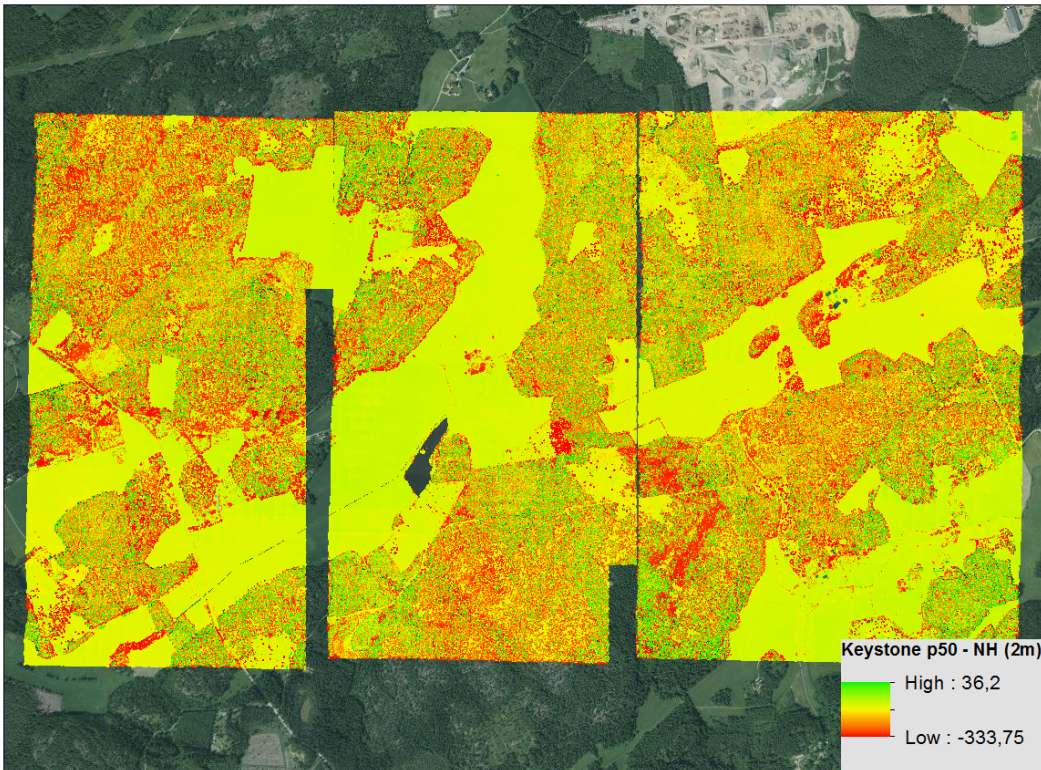


FIGURE 21. CHANGE DETECTION IMAGE BETWEEN THE SURFACE INTERPOLATED WITH THE 50TH PERCENTILE FROM THE KEYSTONE POINT CLOUD AND NNH-SURFACE, RESOLUTION 2 METERS. NO CLASSES.

Figure 21 shows an unedited change detection image. The legend shows that at least one negative outlier exists (-333), the surfaces used for this change detection has not been noise reduced, therefore the outliers are still visible. The extreme value of the outlier is most likely due to a gross mismatch in due to shadows. In the image it can be seen that there is a lot of red, i.e. negative values and it can be expected that these values indicated areas with deforestation. There are green pixels all over the forest areas, indicating positive change detection values and the bare ground feature shows a homogeneous green/yellow color. Probably values close to zero. This image gives an idea of what has happened in the area between the times the surface data was collected, but the information is not very clear.

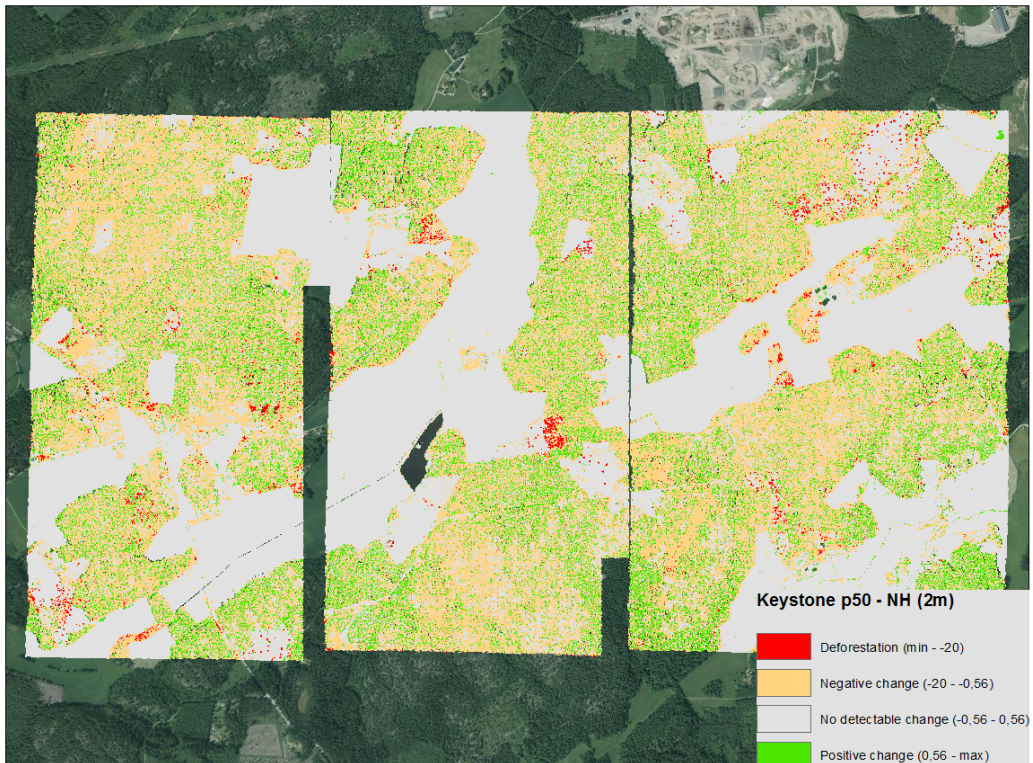


FIGURE 22. CHANGE DETECTION IMAGE BETWEEN THE SURFACE INTERPOLATED WITH THE 50TH PERCENTILE FROM THE KEYSTONE POINT CLOUD AND NNH-SURFACE, RESOLUTION 2 METERS. VALUES ARE CLASSIFIED.

Figure 22 shows the same image as Figure 21 but the values are classified into four classes. In this image, areas with deforestation are clearer, with the largest area in the center of the image standing out the most. This area is indeed an area where the forest has been cut down between the collection dates of the two data sets. Pixels, or smaller areas, labeled as deforestation is sprinkled across the image. These are probably not deforestations but rather outliers or single trees being cut down.

One class is called ‘No detectable change, which is all values within $\pm 2\sigma$ (Table 2). Most areas with the bare ground features are included in that class, which means that no positive or negative change can be detected in those areas. The negative and positive changes are both spread out over the forest feature. It is hard to differentiate where there has been negative or positive change due to the noisy outlook.

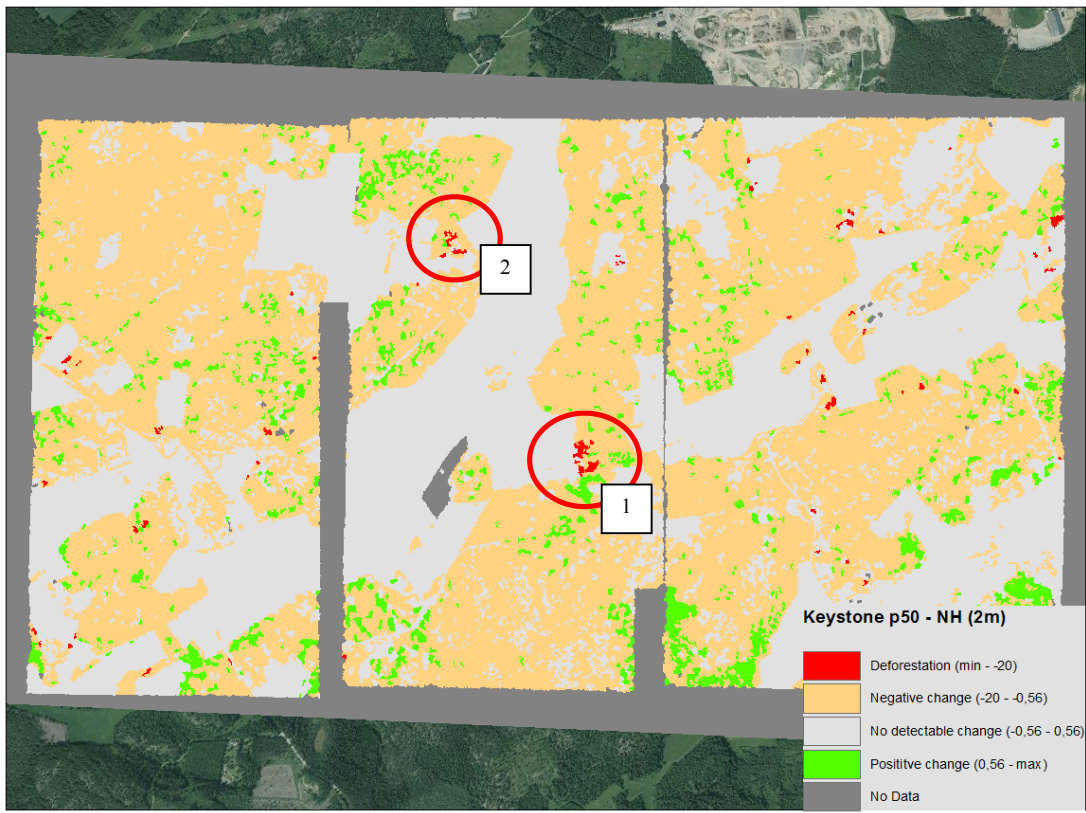


FIGURE 23. CHANGE DETECTION IMAGE BETWEEN A SURFACE INTERPOLATED WITH THE 50TH PERCENTILE FROM THE KEYSTONE POINT CLOUD AND NNH-SURFACE, RESOLUTION 2 METERS. VALUES ARE CLASSIFIED AND SINGLE PIXELS ARE ELIMINATED.

Figure 23 show the same difference image and the same classes as Figure 22, but single pixels, and pixels with less than 20 neighboring pixels of the same class has been eliminated and either replaced by the neighboring class or set to No Data, depending on if the neighboring class is big enough. By viewing the results in this way an overview of the general change of the area can be distinguished. It is shown that most areas with the forest feature have a negative change which is very unlikely. The areas colored in red should be deforestation, which is true for the large area in circle 1, see Figure 24 for deforestation area.



FIGURE 24. DEFORESTATION IN FIGURE 20 CIRCLE 1, THE AREA IN 2011 AND THE AREA IN 2014.

Circle 2 Shows deforestation too, but this area is the same area shown in Figure 12 and Figure 14, an area with deciduous forest that is registered in the NNH point cloud but in none of the image matched point clouds. There are other small areas that are classed as deforestation but in fact are not. It seems like this approach can pin point areas where deforestation has taken

place, but also confuse other areas for deforestation. In the next two Figures it is tested if different resolutions or percentiles can distinguish deforestation better than others.

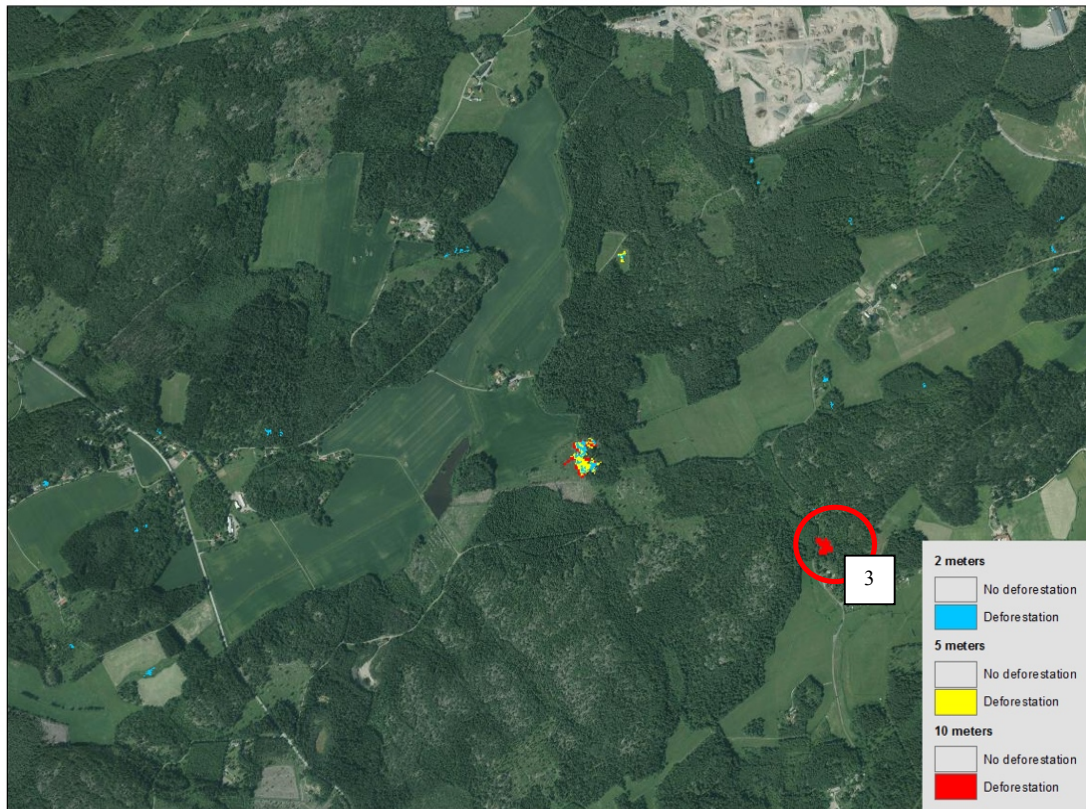


FIGURE 25. CHANGE DETECTION IMAGE BETWEEN THE SURFACES INTERPOLATED WITH THE 50TH PERCENTILE FROM THE KEYSTONE POINT CLOUD AND NNH-SURFACE IN DIFFERENT RESOLUTIONS. ONLY THE DEFORESTATION CLASS IS SHOWN.

Figure 25 shows classified deforestation for the different resolutions. A resolution of 2 meters finds smaller areas across the image. Probably this is due to the fact that a lower resolution allows for more pixels of the same class neighboring each other, whereas a higher resolution has fewer pixels in areas with negative change. The 10-meter resolution finds two areas of deforestations. It finds one area in the center where actual deforestation has taken place and one area circled in circle 3. The second one is not an area where deforestation has taken place; see Figure 26 below for visual.



FIGURE 26. NO DEFORESTATION IN FIGURE 22 CIRCLE 3, THE AREA IN 2011 AND THE AREA IN 2014.

As Figure 26 shows there has been no harvesting of trees in the area, but it looks like there might be leafy trees that has dried out in the image from 2014. This might be the reason for the misconception, much like the deciduous forest shown in Figure 12 and Figure 14.

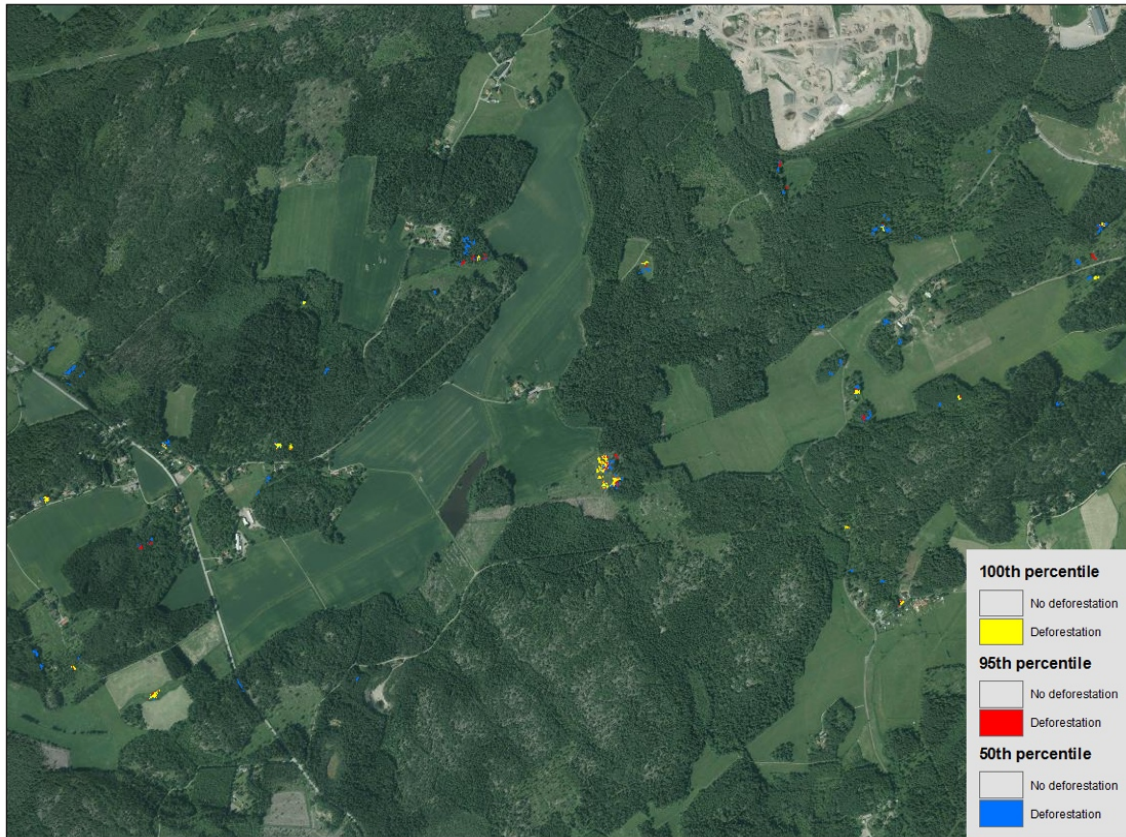


FIGURE 27. CHANGE DETECTION IMAGE BETWEEN THE SURFACES INTERPOLATED WITH THE 50TH, 95TH AND 100TH PERCENTILE FROM THE KEYSTONE POINT CLOUD AND NNH-SURFACE, RESOLUTION 2 METERS.

Figure 27 shows the deforestation detected by different interpolation percentiles. The 50th percentile seems to detect more areas with deforestation than the other percentiles. The 50th percentile will naturally have a slightly lower surface than the other percentiles, especially in areas with forest feature since the variations are greatest there. Since the change is between the interpolated surface and the NNH-surface the negative change will be greater while the positive change will be smaller in comparison to the other percentiles. The 100th and 95th percentile give very similar areas of forestation. All three percentiles find the area with actual deforestation and the 50th percentile find more false areas of deforestation.

7 DISCUSSION

Both Keystone and ERDAS has generated dense point clouds with well-defined features like houses, ditches, roads, trees and fields. One area in particular became an issue for both image matched point clouds (the issue is clearly noticeable in profile views of the area in Figure 12 and Figure 14). The problematic area is shown in Figure 28 and it contains an area with coniferous forest that was not included in either the ERDAS or the Keystone point cloud, but in NNH-point cloud. When viewing the area from the image used for the image matching (Figure 28), it can be seen that there are no leafs on the trees. Instead most of the ground is visible as well as the shadow casted from the tree trunks. As mentioned in 3.2 *Data*, The

images used for image matching were collected in late August 2014 after a hot and dry summer where forest fires occurred in neighboring counties. This might be the reason for the state of the trees in that area. It still shows the inability of the photogrammetric methods to find points in such areas. In the point clouds no other larger areas in with such issue can be found, but that does not exclude that the same issue occurs in smaller scales. This area might be especially vulnerable to the drought and that why it is so clear. But the same thing can occur on areas with only one or a few trees, or maybe a tree has died, then the photogrammetric method might have trouble correctly identifying these features. This also put a time frame of when the images used should have been collected. For instance, imagery taken in early spring before the vegetation has blossomed might cause big issues, as well as imagery taken during late fall and snow free winter time.



FIGURE 28. DECIDUOUS FOREST IN STUDY AREA THAT ISN'T INCLUDED IN THE PHOTOGRAHMETRIC GENERATED POINT CLOUDS

In Figure 15 a profile view of the ERDAS point cloud and the NNH point cloud can be seen over an area with forest feature and some bare ground. It can be seen that the image matched point cloud can find point in between trees in dense forests. This is naturally due to the fact that a point needs to be visible from two overlapping images, i.e. two angles. The further down in between tree tops it's harder to see from two views. Also, if the forest is dense there might not be a view from any angle since the trees are covering the sight. This in comparison to LiDAR data is a shortcoming if one wants to, for instance, measure the density of a forest. However, for generating a surface it is not necessarily an issue. Since a surface should represent the height of the ground and the features on top of it, it is not as interesting to know how the forest looks underneath the treetops. Figure 15 also displays dense point cloud matching in the treetops and it appears that the image matched point cloud is a bit higher than the NNH point cloud.

Several surfaces were created from the two image matched point cloud with different resolutions and different interpolations percentiles. In both Chart 1 and Chart 2, but most prominently in Chart 2, it can be seen that a higher resolution is more affected by the change of interpolation percentiles, the higher the resolution the lesser the surface is affected by the percentile. This means that higher resolutions are more stable than lower resolutions, i.e. a surface with a resolution of 2 meter is less affected by the percentiles than a surface with a resolution of 10 meters. Also, when interpolating with a lower resolution more points are used for each grid cell resulting in every point having lower influence. So the difference between interpolating with lower percentiles and the 100th percentiles are bigger for lower resolutions than for higher one, which can be seen clearly with the Keystone data in Chart 1.

Surfaces interpolated with the 100th percentiles show the biggest increase in change in both Chart 1 and Chart 2. Surfaces interpolated with the 100th percentile include all positive outliers in the point cloud. When subtracting the point cloud value from the surface value, the resulting value will be higher if a higher percentile was used for the interpolation. Therefore, using the 100th percentile that also includes possible gross outliers will give a distinctively higher value.

Figure 17 visualize how the different percentiles affect the surface and Figure 18 visualizes how the different resolutions affect the surface. It is not surprising that the different percentiles generate similar surfaces but with slightly different heights. The question to be answered is which one gives the most accurate height. The lower percentiles catch the variation in height better than the higher one, and as established the 100th percentile include positive outliers.

A tilt-check was done for each image matched point cloud. Since any systematic error in the surfaces would be a result of a systematic error in the point cloud, only one surface from each point cloud need to be checked. If there would have been any systematic tilt, the same tilt would be found in all surfaces generated from that point cloud. Any tilting could be found for neither of the tested surfaces, hence no systematic tilt could be found in either of the point clouds.

In order to find any continuous height error, ground truth data in form of snippets from flat roads with no nearby trees was used. The GTD was intersected with the difference images of the generated surfaces subtracted with the NNH-surface. The statistics from these areas are shown in Table 2. In the table the mean value for each surface is shown. The mean would, if it is anything but zero, indicate a continuous height error. However, due to random variations it can be expected that values within the range of +/- 2 σ are natural variations from zero. Therefore, with regards to the random variations no continuous height error is detected.

Table 2 show that the random error range is wider for lower resolutions. The reason for this might be that the size of each GTD segment is smaller than the size of the pixels in the lower resolutions, as seen in Figure 29. Therefore, no pixels in the lower resolutions are completely covered by the GTD segments hence the surrounding areas affect the pixel values of the pixels intersecting with the GTDs. If it would be possible to have bigger GTD areas that would solve this problem. This could have been done by having another control data set for GTDs and other accuracy estimations.

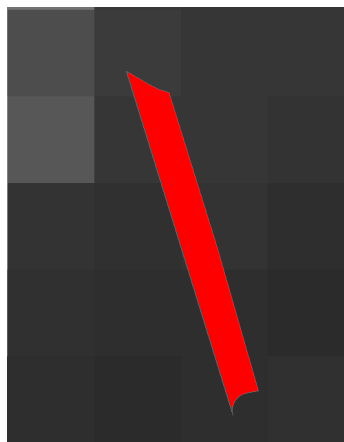


FIGURE 29. ONE GTD SEGMENT OVER A SURFACE WITH 10-METER RESOLUTION

Chart 3 shows the median of the difference between the surfaces and the reference point cloud (NNH) for the bare ground feature and Chart 4 shows the same for the forest feature. In Chart 3 the y-axis is on a decimeter-scale and many of the values are within the +/- 2 σ range. This means that it is hard to draw any conclusion of the change in the bare ground.

The y-axis in Chart 4 has intervals on a meter-level, meaning the change found in the forest feature is larger than the change found in the bare ground feature. The 50th percentile finds negative change; the 100th percentile finds positive change and the 90th and 95th finds almost no change at all. The conclusion that can be withdrawn from this is that in areas with forest feature where no change has occurred, the 50th and 100th percentile for the lower resolutions indicates a great deal of change anyways. The 90th and 95th percentiles accurately displays almost no change. The 2-meter resolution for the 50th and the 100th also show quite a low level of change, indicating that the results from the 2-meter resolution gives a more reliable result than the lower resolutions.

Table 1 shows the accuracy of the ERDAS- and Keystone-point clouds in comparison to the reference NNH-point cloud. The accuracy is divided into the two features, bare ground and forest. It can be seen that the difference between the accuracy of the features is big. The photogrammetric point clouds have a low accuracy in areas with forest feature and good accuracy in areas with bare ground. As mentioned earlier the forest feature contains a lot of noise, due to mismatches, moving treetops and shadows. The accuracy for the generated surfaces in comparison to the reference NNH-point cloud is shown in Table 3 for the bare ground feature and Table 4 for the forest feature. The tables show that the accuracy for the bare ground feature does not improve with the interpolation of the point cloud but the forest feature does. The accuracy of the forest feature also improves with a lower resolution, meaning that interpolating a point cloud with forest feature will improve the accuracy for every cell when using lower resolutions. Still, the accuracy is unacceptably low. Table 5 show noise reduced surfaces from the Keystone point cloud interpolated with the 100th percentile. The accuracy has nearly doubled from the corresponding surfaces that has not been noise reduced. To apply some kind of noise reducing filter on the point cloud is often done, however not in this thesis, but Table 5 shows that by doing so the result will improve significantly. The result in Table 5 gives hope for this method to be used for generating surface models.

In chapter 6.3.4 *change detection* visualizations of change detection are presented. It can be seen that the change detection image without any classification (Figure 21) indicates a lot of areas that appear to have changed. When classified according to the 95% confidence interval and the knowledge that forest exploitation commonly takes place on trees taller than 20 meters the areas indicated as deforestation is trimmed down (Figure 22). However, the image is quite scattered with the classes. In Figure 23 the data is ‘evened out’ in order to eliminate single pixels and give it a more homogeneous appearance. Now it is easy to find the areas that are suggested to have been deforested. In Figure 23 there are two areas that stand out as deforestations. One of the areas (Figure 23 circle 1) is in fact deforestation (Figure 28) and the other area (Figure 23 circle 2) is not. The second area is the deciduous forest shown in Figure 12 and Figure 14, where both ERDAS and Keystone fails to register the forest.

Figure 25 and Figure 27 shows how different interpolation percentiles and resolutions on the surfaces affect the change that can be found. It focuses solely on finding areas of deforestation. It shows that a lower resolution will give more homogeneous areas, but in Figure 25 circle 3 the 10-meter resolution faulty points out an area for deforestation that no other resolution does. It seems like the higher resolutions find smaller areas of deforestation. Furthermore, the data used in this thesis is just two different data sets. In order to see how well the photogrammetric method work in producing point clouds within the different features there should be one data set for accuracy assessment and another for the change analysis. Now the GTDs was chosen on small parts of roads that is known to not have changed in the time between the data sets were collected. If LiDAR data would have been collected close to the time the optical imagery was collected it would be easier to distinguish the error caused by the method from the actual change. Since it has been three years in between the collection of

the datasets and one dataset was collected in late spring and the other in late summer there should be small changes. The crop in the fields might be in different growing phases and the forests have grown in both heights and volume. Now it looks like the 90th and 95th gives the best result for the forest feature according to Chart 4, but since there could have been growth of the forest maybe the 100th percentile that shows growth is more accurate.

The best accuracy found in Table 1 is found for the surface interpolated with the 50th percentile and 2-meter resolution from the ERDAS point cloud, it has a +/- 2σ . of 0.54 meters. In comparison to the height accuracy of NNH grid 2+, which is higher than 0.5 meter, it is not too bad. This accuracy only applies to flat hard surfaces (the GTDs), and the accuracy for hard surfaces in the NNH grid 2+ is at least 0.1 meters. This means that the accuracy attained in this thesis does not compare to the accuracy in a LiDAR generated point cloud.

8 CONCLUSIONS

The point clouds generated through image matching are dense and do a good job at following the overall profile of the surface. Both software used failed to register an area with deciduous forest where the leafs seem to have either fallen off or dried up. This put a constraint on the collection period of when the imagery used can be collected.

The photogrammetric method misses points in between trees in dense forests. However, when interpolating a surface model this is not a big issue since the general height of the forest is interesting. If this method was to be used for example to measure the volume or density of the forest this might be an issue, but in this thesis the important feature is the height of the forest. The surfaces are highly affected by the different interpolation percentiles. The 100th percentile include outliers and are therefore more affected by the change of resolution. In a lower resolution gross outliers have a bigger influence since the cell it represents is larger. This also means that lower resolutions are more affected by the different interpolation percentiles than the higher resolutions.

The accuracy of the forest feature improves when interpolated with a lower resolution. When the surface is noise reduced the accuracy improves significantly, making the exclusion of noise and gross outliers vital to generate accurate surfaces.

According to the GTDs the most accurate surface is the one interpolation from the ERDAS point cloud with a resolution of 2 meters and an interpolation percentile of 50. When looking at the forest feature it seems like the 90th or the 95th percentiles give the most accurate result but due to uncertainties regarding the amount of growth in the forest this can not be completely established.

9 RECOMMENDATIONS AND FUTURE STUDIES

This thesis has stumbled on to some issues that could have been discarded if certain knowledge had been known in an earlier stage. There are also some thoughts that would be interesting to try out and work that can enhance the result of this thesis.

In this thesis the same data was used for both accuracy determination and change analysis. If possible, having a separate data set close in time for accuracy determination would be preferable. Having two separate data sets allows a more stable analysis of the two different features, bare ground and forest. Of course the data that is available is limited if the researcher, like in this case, are dependent on the grace of others to receive data. Often municipalities in Sweden collect optic airborne imagery quite regularly and therefore it might be possible to receive two sets of images, one set close to the time the LiDAR data was collected and one set earlier or later to be used for change detection. Of course the conditions

of the imagery in terms of flying height, maybe different sensors and collection time during the year will cause the point clouds to have slightly different accuracies. A study on how the properties change in the point cloud when using imagery with different properties would be interesting too. The other option is to receive LiDAR data that the municipality have collected themselves, but it is usually done less frequently.

It would also be interesting to investigate how the image matched point clouds can be manipulated in order to give a higher accuracy. For instance, the LiDAR point cloud can be used to even out the surfaces by taking the height and position of points in the point cloud and use them to “even out” the surface. Using the points as true heights and re-interpolate the surface to fit the points. Another way to do this can be to manually identify gross outliers in the image matched point clouds and take them away before interpolation the surfaces. A test to eliminate gross outliers and noise was conducted in this thesis, showing that noise reduction improves the result considerably. Therefore, in future studies noise reduction of the point clouds are recommended. Other ways of reducing noise can be explored. For instance, if there is no reference surface at hand gross outliers can be eliminated by setting a limit value based on the deviation from the surface mean value.

REFERENCES

- Barazzetti, L., n.d. *Matching of Satellite, Areal and close-range Images*. [Online] Available at: <http://www2.le.ac.uk/departments/physics/research/eos/format-eo/lecture-notes/matching-of-satellite-aerial-and-close-range-images> [Accessed 5 february 2016].
- Barnard, S. T. & Thompson, W. B., 1980. Disparity analysis of images. *IEE Transactions on pattern analysis and machine intelligence*, July, pp. 333-340.
- Boberg, A., 2013. Digitala höjdmodeller. In: *Geodetisk och fotogrammetrisk mätnings- och beräkningsteknik*. Stockholm: Lantmäteriet et. al, pp. 243-245.
- Boberg, A., 2013. Fotogrammetriska metoder. In: *Geodetisk och fotogrammetrisk mätnings- och beräkningsteknik*. Stockholm: Lantmäteriet et.al., pp. 204-220.
- Boberg, A., 2013. Geodetisk och fotogrammetrisk mätnings- och beräkningsteknik. Stockholm: Lantmäteriet et. al, pp. 257-280.
- Boberg, A., 2013. Laserskanning. In: *Geodetisk och fotogrammetrisk mätnings- och beräkningsteknik*. Stockholm: Lantmäteriet et. al, pp. 257-280.
- Dall'asta, E. & Roncella, R., 2014. *A comparison of semiglobal and local dense matching algorithms for surface reconstruction*. Riva del Garda, Italy, The internaional Archinves of the Photogrammetry, Remote sensing and Spatial information Science.
- ERDAS Imagine, n.d. *purdue.edu*. [Online] Available at: <ftp://ftp.ecn.purdue.edu/jshan/86/help/html/import export/import patb.htm#ori> [Accessed 21 may 2016].
- Esri, 2011. *ArcGIS Desktop 9.3 Help*. [Online] Available at: <http://webhelp.esri.com/arcgisdesktop/9.3> [Accessed 10 05 2016].
- Förstner, W., 1984. *A feature based correspondence algorithm for image matching*. Rovaniemi, Inst. Arch. of Photogrammetry, p. 17.
- Förstner, W. & Gulch, E., 1987. *A fast operator for detection and precise location of disticnt points, corners and centres of circular features*, Interlaken: ISPRS Intercommission.
- Fischler, M. A. & Robert, B. C., 1981. Random Sample Consensus: A Paradigm for Model Fitting with Apphcations to Image Analysis and Automated Cartography. *Graphics and Image Processing*, 24(6), pp. 381-395.
- Fugro Geospatial, 2016. *fugroviewer*. [Online] Available at: www.fugroviewer.com
- Gehrke, S., et al., 2010. *Semi-Global Matching: An alternative to LiDAR for DSM generation?*, s.l.: Commission I.
- Geografiska Sverigedata, 2015. *Produktbeskrivning: GSD-Höjddata, grid 2+*, s.l.: Lantmäteriet.

GeoXD AB, 2015. *Produktion av ytmödeller med hjälp av bildmatchning*, Stockholm: Lantmäteriet.

Haala, N., 2009. *Comeback of Digital Image Matching*. Wichmann Verlag, Heidelberg, Dieter Fritsch, p. 13.

Haala, N., 2014. Dense Image Matching Final Report. *EuroSDR*, pp. 115-143.

Harris, C. & Stephens, M., 1988. *A combined corner and edge detector*, Plessey: The Plessey Complany plc..

Hexagon Geospatial, 2015. *Erdas Imagine Brochure*. [Online]
Available at: [ERDAS Imagine](#)

Hexagon geospatial, 2016. *about Hexagon Geospatial*. [Online]
Available at: <http://www.hexagongeospatial.com/>

Hexagon geospatial, 2016. *Imagine photogrammetry*. [Online]
Available at: <http://www.hexagongeospatial.com/>

hexagongeospatial, 2015. *ERDAS Imagine help*. [Online]
Available at: <https://hexagongeospatial.fluidtopics.net>
[Accessed 10 5 2016].

Hirschmüller, H., 2008. Stereo Processing by Semiglobal Matching and Mutual Information. *IEEE Transactions on Pattern Analysis and Machine Intelligence (Volume:30, Issue: 2)*, pp. 328-341.

Hirschmüller, H., 2011. *Semi-Global Matching – Motivation, Developments and Applications*. Oberpfaffenhofen, Wichmann/VDE Verlag, Berlin & Offenbach, pp. 173-184.

Horemuz, M., 2015. *Air-borne laser scanning*. Stockholm: Royal Institute of Technology.

Humenberger, M., Engelke, T. & Kubinger, W., 2010. *A census-based stereo vision algorithm using modified semi-global matching and plane fitting to improve matching quality*. San Fransisco, IEEE, pp. 77-84.

James, D., Eckermann, J., Belblidia, F. & Sienz, J., 2015. *Point cloud data from Photogrammetry techniques to generate 3D Geometry*. Swansea, ReserchGate, pp. 343-348.

King, A., 1989. Inertial Navigation - Forty years of evolution. *GEC Review*, 13(3), pp. 140-149.

Lantmäteriet, 2016. *Kartor och geografisk information; Höjddata; GSD-Höjddata, grid 2+*. [Online]
Available at: <http://www.lantmateriet.se>
[Accessed 02 03 2016].

Lantmäteriet, 2016. *Kartor och geografisk information; Höjddata; Laserdata*. [Online]
Available at: <https://www.lantmateriet.se>
[Accessed 27 04 2016].

Lantmäteriet, 2016. *Lantmäteriet*. [Online]
Available at: <http://www.lantmateriet.se>
[Accessed 20 may 2016].

Leberl, F. et al., 2010. Point clouds: Lidar versus 3D Vision Vol.76, No. 10. October, pp. 1123-1134.

Mattecentrum, 2016. *Standardavvikelse*. [Online]
Available at: www.matteboken.se
[Accessed 11 08 2016].

Metria, 2016. *Metria*. [Online]
Available at: <http://www.metria.se>
[Accessed 20 may 2016].

Philpot & Philipson, 2012. Remote sensing fundamentals. In: *Remote sensing fundamentals*. Cornell: Cornell University, p. 7. Photogrammetry.

Rapidlasso GmbH, 2016. *lastools*. [Online]
Available at: <http://rapidlasso.com>
[Accessed 10 04 2016].

Scharstein, D. & Szeliski, R., 2001. A Taxonomy and Evaluation of Dense Two-Frame. *Stereo and Multi-Baseline vision*, pp. 131-140.

Schenk, T., 2005. Introduction to Photogrammetry. In: *Introduction to Photogrammetry*. Columbus(Ohio): The Ohio state university, pp. 16-19.

Shapiro, L. S. & Brady, J. M., 1992. Feature-based correspondence: an eigenvector approach. *Image and vision computing*, 5 june, pp. 282-288.

SMHI, 2014. *SMHI*. [Online]
Available at: www.smhi.se
[Accessed 21 may 2016].

Spacemetric, 2016. *Keystone enterprise*. [Online]
Available at: www.spacemetric.com
[Accessed 10 04 2016].

Szeliski, R., 2011. Image processing. In: *Computer Vision: Algorithms and Applications*. New York: Springer - Verlag London, p. 153.

Szeliski, R., 2011. Stereo correspondence. In: *Computer Vision: Algorithms and Applications*. New York: Springer-Verlag London, p. 484.

Wehr, A. & Lohr, U., 1999. Airbotne laser scanning - an introduction and overview. *ISPRS journal of photogrammetry and remote sensing*, pp. 68-82.

Westoby, M.J., et al., 2015. 'Structure-from-Motion' photogrammetry: A low-cost, effective tool for geoscience applications. *Geomorphology*, 15 december, pp. 300-314.

Reports in Geodesy and Geographic Information Technology

The TRITA-GIT Series - ISSN 1653-5227

- 16-001 **Marvin McCutchan.** Investigation of Geoid Changes in Northern Europe Using Latest Data from the Dedicated Satellite Gravity Mission GRACE. Master of Science thesis in Geodesy No. 3141. Supervisor: Huaan Fan. January 2016.
- 16-002 **Alice Tourtier.** Study of the contribution of an ionospheric model embedded on a dual frequency receiver. Master of Science thesis in Geodesy No. 3142. Supervisors: Anna Jensen (KTH), Marion Aubault and Sébastien Rougerie (CNES). February 2016.
- 16-003 **Shinan Wang.** Detection and Analysis of GNSS Multipath. Master of Science thesis in Geodesy No. 3143. Supervisor: Anna Jensen. June 2016.
- 16-004 **Felicia Steinvall.** Implementation av Svensk geoprocess i kommunal verksamhet. Master of Science thesis in Geoinformatics. Supervisors: Erik Persson, Agima Management and Gyöző Gidofalvi. June 2016.
- 16-005 **Anna Österman.** Lokaliseringssmodellen location-allocation som beslutsunderlag för biblioteksplanering. Master of Science thesis in Geoinformatics. Supervisors: Monika Sjölund, Sweco Position and Jan Haas, KTH. June 2016.
- 16-006 **Manuela Alvarez.** Mapping forest habitats in protected areas by integrating LiDAR and SPOT Multispectral Data. Master of Science thesis in Geoinformatics. Supervisors: Torbjörn Rost, Metria and Yifang Ban, KTH. June 2016.
- 16-007 **Ehsan Saqib.** Anonymous Mobile Consumer Analysis Platform. Master of Science thesis in Geoinformatics. Supervisor: Gyöző Gidofalvi. June 2016.
- 16-008 **Anders Magnusson.** Web Application for Travel Diary Annotation and Methods for Trip Destination and Purpose Inference. Master of Science thesis in Geoinformatics. Supervisor: Gyöző Gidofalvi. June 2016.
- 16-009 **Rebecca Ilehag.** Exploitation of Digital Surface Models from Optical Satellites for the Identification of Buildings in High Resolution SAR Imagery. Master of Science thesis in Geoinformatics. Supervisors: Stefan Auer, DLR and Yifang Ban, KTH. June 2016.
- 16-010 **Ella Syk and Fredrik Hilding.** User-centric Web-based System for Visualization of NIS-data for Layman Users. Master of Science thesis in Geoinformatics. Supervisors: Axel Brønder, DigPro and Gyöző Gidofalvi. June 2016.
- 16-011 **Liene Some.** Automatic image based road crack detection methods. Master of Science thesis in Geodesy No. 3144. Supervisors: Johan Vium Andersson, WSP and Milan Horemuz, KTH.
- 16-012 **Joline Bergsjö.** Photogrammetric point cloud generation and surface interpolation for change detection. Master of Science thesis in Geodesy No. 3145. Supervisors: Torbjörn Rost, Metria and Milan Horemuz, KTH.

TRITA-GIT EX 16-012

ISSN 1653-5227

ISRN KTH/GIT/EX--16/012-SE

TRITA GIT EX 16-012
ISSN 1653-5227
ISRN KTH/GITEX--16/012-SE